

World Small Animal Veterinary Association Renal Pathology Initiative: Classification of Glomerular Diseases in Dogs

Veterinary Pathology
2016, Vol. 53(1) 113-135
© The Author(s) 2015
Reprints and permission:
sagepub.com/journalsPermissions.nav
DOI: 10.1177/0300985815579996
vet.sagepub.com



R. E. Cianciolo¹, F. C. Mohr², L. Aresu³, C. A. Brown⁴, C. James⁵,
J. H. Jansen⁶, W. L. Spangler⁷, J. J. van der Lugt^{8,9}, P. H. Kass¹⁰,
C. Brovida¹¹, L. D. Cowgill¹², R. Heiene¹³⁻¹⁵, D. J. Polzin¹⁶,
H. Syme¹⁷, S. L. Vaden¹⁸, A. M. van Dongen⁹, and G. E. Lees¹⁹

Abstract

Evaluation of canine renal biopsy tissue has generally relied on light microscopic (LM) evaluation of hematoxylin and eosin-stained sections ranging in thickness from 3 to 5 μm . Advanced modalities, such as transmission electron microscopy (TEM) and immunofluorescence (IF), have been used sporadically or retrospectively. Diagnostic algorithms of glomerular diseases have been extrapolated from the World Health Organization classification scheme for human glomerular disease. With the recent establishment of 2 veterinary nephropathology services that evaluate 3- μm sections with a panel of histochemical stains and routinely perform TEM and IF, a standardized objective species-specific approach for the diagnosis of canine glomerular disease was needed. Eight veterinary pathologists evaluated 114 parameters (lesions) in renal biopsy specimens from 89 dogs. Hierarchical cluster analysis of the data revealed 2 large categories of glomerular disease based on the presence or absence of immune complex deposition: The immune complex-mediated glomerulonephritis (ICGN) category included cases with histologic lesions of membranoproliferative or membranous patterns. The second category included control dogs and dogs with non-ICGN (glomerular amyloidosis or focal segmental glomerulosclerosis). Cluster analysis performed on only the LM parameters led to misdiagnosis of 22 of the 89 cases—that is, ICGN cases moved to the non-ICGN branch of the dendrogram or vice versa, thereby emphasizing the importance of advanced diagnostic modalities in the evaluation of canine glomerular disease. Salient LM, TEM, and IF features for each pattern of disease were identified, and a preliminary investigation of related clinicopathologic data was performed.

¹Department of Veterinary Biosciences, College of Veterinary Medicine, The Ohio State University, Columbus, OH, USA

²Department of Pathology, Microbiology, and Immunology, School of Veterinary Medicine, University of California, Davis, CA, USA

³Facoltà di Medicina Veterinaria, Dipartimento di Biomedicina comparata e Alimentazione, Università di Padova, Legnaro, Italy

⁴Athens Veterinary Diagnostic Laboratory, College of Veterinary Medicine, University of Georgia, Athens, GA, USA

⁵IDEXX Laboratories, Ltd., Wetherby, United Kingdom

⁶Department of Basic Sciences and Aquatic Medicine, Norwegian University of Life Sciences, Oslo, Norway

⁷NSG Pathology, Davis, CA, USA

⁸IDEXX Europe, BV, Hoofddorp, The Netherlands

⁹Department of Clinical Sciences of Companion Animals, Faculty of Veterinary Medicine, Utrecht University, Utrecht, The Netherlands

¹⁰Department of Population Health and Production, School of Veterinary Medicine, University of California, Davis, CA, USA

¹¹ANUBI Ospedale per Animali da Compagnia, Moncalieri, Italy

¹²Department of Medicine and Epidemiology, School of Veterinary Medicine, University of California, Davis, CA, USA

¹³Blue Star Animal Hospital, Gothenburg, Sweden

¹⁴PetVett Dyresykehus, Oslo, Norway

¹⁵Department of Companion Animal Clinical Sciences, Norwegian University of Life Sciences, Oslo, Norway

¹⁶Department of Veterinary Clinical Sciences, College of Veterinary Medicine, University of Minnesota, St Paul, MN, USA

¹⁷Department of Clinical Sciences, Royal Veterinary College, Hatfield, UK

¹⁸Department of Clinical Sciences, College of Veterinary Medicine, North Carolina State University, Raleigh, NC, USA

¹⁹Department of Small Animal Clinical Sciences, College of Veterinary Medicine and Biomedical Sciences, Texas A&M University, College Station, TX, USA

Supplemental material for this article is available on the Veterinary Pathology website at <http://vet.sagepub.com/supplemental>.

Corresponding Author:

R. E. Cianciolo, Department of Veterinary Biosciences, College of Veterinary Medicine, The Ohio State University, Columbus, OH, USA.

Email: cianciolo.14@osu.edu

Diagnosis of canine glomerular disease has been based, in part, on the World Health Organization classification system created to define and standardize the categories of human glomerular disease.* Although human glomerular disease is routinely defined following (1) examination of thin (3 μm) light microscopic (LM) sections viewed with a specific panel of histochemical stains, (2) immunofluorescence (IF) to detect the presence of immunoglobulins and complement components, and (3) transmission electron microscopy (TEM), this has generally not been the case with diagnosis and classification of glomerular disease in dogs.[†] Moreover, it is apparent that although canine glomerular diseases share many of the structural characteristics seen in their human counterparts, there are striking differences as well. The infrequent use of advanced diagnostic modalities and the uncertainty regarding the accuracy of a diagnosis based solely on histopathology have created concerns regarding the clinical utility of canine renal biopsy. Furthermore, the dearth of peer-reviewed literature examining epidemiologic, therapeutic, and outcome factors in dogs with spontaneous glomerular disease can be partly explained by the nonstandardized, often retrospective, analysis of renal tissue by veterinary pathologists.

To address these concerns, the World Small Animal Veterinary Association–Renal Standardization Study Group (WSAVA-RSSG) was conceived at Netherland's Utrecht University in January 2005.^{13,25} This international group of veterinary nephrologists and pathologists set out to design a study that would develop a comprehensive understanding of glomerular disease in dogs by routinely using standardized LM, IF, and TEM methods to evaluate renal biopsies and by associating the pathologic findings with detailed clinical and case outcome data. Two veterinary diagnostic renal pathology centers—1 in the United States and 1 in Europe—were established to perform the evaluations and facilitate the collection of cases for prospective studies. The US center—created in 2005 at Texas A&M University as the Texas Veterinary Renal Pathology Service—was reorganized in 2013 as the International Veterinary Renal Pathology Service and now operates as a joint effort between The Ohio State University and Texas A&M University. The Utrecht Veterinary Nephropathology Service began examining renal biopsies at Utrecht University, The Netherlands, in 2008. The Utrecht Veterinary Nephropathology Service currently works in cooperation with the Department of Comparative Biomedicine and Food Science at the University of Padova, Italy. The International Veterinary Renal Pathology Service and Utrecht Veterinary Nephropathology Service demonstrated that canine renal biopsies could be evaluated with LM, IF, and TEM in a reasonable diagnostic workflow to provide timely and useful information to clinicians.¹¹

The goals of this study were as follows:

- first, development of a digital pathology platform to allow WSAVA-RSSG pathologists in widely dispersed geographic locations to communicate and collaborate effectively—

through that platform, digitized LM slides and IF and TEM images could be remotely accessed and evaluated by individuals and by the group during online meetings;

- second, development of succinct definitions and scoring criteria for glomerular, tubular, interstitial and vascular lesions; and
- third, use of hierarchical cluster analysis to objectively identify common patterns of glomerular injury in dogs to create a simplified, reproducible, and accurate guide for veterinary pathologists to use when evaluating renal biopsies from dogs with proteinuric renal disease.

Materials and Methods

Case Selection

Dogs in this study had renal biopsies performed because they exhibited proteinuria indicative of the presence of glomerular disease—that is, persistent renal proteinuria with urine protein:creatinine ratio (UPC) values ≥ 2.0 —which was subsequently confirmed by biopsy findings.²³ Additionally, a case had to have biopsy specimens sufficient for diagnosis—specifically, either LM, TEM, and IF findings or LM and TEM findings without IF findings if the LM and TEM findings alone were conclusive. Last, 5 dogs without clinicopathologic indications of renal disease were chosen from the Texas Veterinary Renal Pathology Service database to serve as controls. These dogs were racing Greyhounds from which renal biopsies were performed during ovariohysterectomy prior to adoption as pets.⁴⁵

Clinical Data

Dogs with glomerular disease exhibited a diverse spectrum of clinical illnesses that had been evaluated and treated in various ways before their renal biopsies were obtained. Detailed analysis of the clinicopathologic features of the illnesses exhibited by the dogs was beyond this study's scope, which focused on developing a prototype method for classification of canine glomerular diseases based on pathologic features. Nevertheless, several key clinical laboratory findings provided by submitting veterinarians were compiled for each dog. These findings included magnitude of proteinuria (defined as the highest UPC value observed before biopsy), serum creatinine concentration (SCr; defined as the last value observed before biopsy), and serum albumin concentration (SAlb; defined as the lowest value observed before biopsy). Also, the presence or absence of hypertension was evaluated with the clinical laboratory data; hypertension was defined as a recorded systolic value consistently >160 mm Hg before biopsy or as treatment with any antihypertensive medication (other than an ACE inhibitor drug alone) at the time of biopsy.

Light Microscopy

All specimens for LM evaluation were immersion fixed in 10% buffered formalin, processed, and embedded in paraffin. Tissues were serially sectioned at least 10 times at 3- μm thickness

*References 10, 12, 16, 17, 20, 22, 24, 27, 31–33, 38, 42, 44, 49, 50, 52, 54

†References 10, 12, 20, 24, 32, 33, 38, 44, 50, 54

and stained with hematoxylin and eosin, periodic acid–Schiff reagent (PAS), Masson trichrome (TRI), and the Jones methenamine silver method (JMS). Additionally, thicker (8 μm) sections were cut from at least 1 cortical specimen and stained with Congo red. All histochemical procedures were performed using established methods.

Transmission Electron Microscopy

TEM was performed at the Texas Heart Institute (Houston, TX, USA) and at the Department of Comparative Biomedicine and Food Science, University of Padova, using similar techniques. Briefly, renal tissue containing glomeruli was fixed in chilled 3% phosphate-buffered glutaraldehyde. Specimens were post-fixed in 1% osmium tetroxide, serially dehydrated, infiltrated in an acetone/epoxy plastic, and embedded in plastic. In 1 dog, glomeruli were not present in the glutaraldehyde-fixed sample. For that case, the paraffin-embedded tissue from the LM specimen was harvested, postfixed in 1% osmium tetroxide, and embedded in EM BED 812 and Araldite (Electron Microscopy Sciences, Fort Washington, PA, USA). Plastic blocks were cut with a Sorvall MT2-B ultramicrotome. Thick sections (1 μm) were stained with toluidine blue. These sections were evaluated and appropriate areas identified for thin sectioning. Thin sections were cut at silver-grey interference color (55–60 nm) and placed on copper mesh grids. Grids were stained with uranyl acetate and lead citrate and examined with a JEOL-TEM-1230 transmission electron microscope, and digital photomicrographs were obtained.

Immunofluorescence

Tissues were immersed in chilled Michel's Transport Medium (Newcomer Supply, Middleton, WI, USA) for up to 72 hours during transport to the pathology laboratory, where they were washed 3 times in Michel's Wash (Newcomer Supply, Middleton, WI, USA), placed in plastic cryomolds filled with Tissue-Tek OCT embedding compound (Electron Microscopy Sciences, Fort Washington, PA, USA), and snap-frozen in liquid nitrogen. Blocks were stored at -80°C until sectioned. Thin (4 μm) cryosections were cut on a Leica CM 1850 UV cryostat (Bannockburn, IL, USA) and stored at -80°C until thawed for 1 hour at room temperature for staining. Sections were fixed for 5 minutes in cold 100% acetone, air-dried for 1 hour, then rehydrated in phosphate-buffered saline. Direct IF was performed with fluorescein isothiocyanate-conjugated polyclonal goat anti-dog IgG, IgM, IgA, and C3 antibodies (Bethyl Labs, Montgomery, TX, USA), as well as with fluorescein isothiocyanate-conjugated polyclonal rabbit anti-human C1q, kappa light chain, and lambda light chain antibodies (Dako North America, Carpinteria, CA, USA). Sections were incubated for 1 hour with an appropriate dilution of each antibody, then washed with phosphate-buffered saline. Sections were coverslipped using a mounting medium that retarded fluorescence quenching (Prolong Gold, Invitrogen, Carlsbad, CA, USA) and were examined using appropriate filters with an epifluorescence microscope (Olympus, Center Valley, PA, USA).

Image Acquisition and Viewing

Renal biopsies prepared for LM were digitally scanned with a slide-scanning instrument (ScanScope CS, Aperio, Vista, CA, USA). Scanned slides along with digitized TEM and IF images were stored and managed by digital pathology software (Spectrum, Aperio) for review (ImageScope CS and WebScope, Aperio), by individual pathologists and during group conferences (GoToMeeting, Citrix Systems, Inc., Santa Barbara, CA, USA). Specifically, digital images from all 3 modalities were reviewed and graded independently by all 8 pathologists prior to group discussions.

Scoring

For each of the 3 methods of examination, changes in the renal tissue were deconstructed to their most basic components, which were then discussed by the pathologists to formulate the most appropriate way to assess each lesion. Some lesions were scored as present or absent, whereas others were given a severity grade. These discussions also facilitated the clarification of descriptive terms for the various lesions (Supplemental Table 1). This process produced the LM, TEM, and IF scoring schemes described below. Pathologists filled out an electronic evaluation form for each case. Scores were collated by a single pathologist (R.E.C.), and averages or consensus scores were used for data analysis, as discussed below.

LM. The histologic features evaluated are listed in Supplemental Table 2. Two different grading schemes were required to assess distribution and severity of features. One set of lesions was scored on the basis of whole slide evaluations of glomerular, interstitial, and vascular compartments. These lesions were scored on a scale of 0–4 representing different degrees of intensity—*not present*, *present but rare*, *mild*, *moderate*, and *severe*, respectively. In instances of general agreement on the survey, the average score was used for statistical analysis; however, consensus scores (based on discussions during online conferencing sessions) were used for the occasional instances in which survey responses varied widely. The second set of lesions was scored by evaluating individual glomeruli (4–32 glomeruli per case) and individual fields of tubulointerstitium, measuring $400 \times 600 \mu\text{m}$ (5–32 fields per case) to detect focal lesions. Each pathologist graded a set of unique glomeruli and tubulointerstitial fields. Scores were reported as percentage of glomeruli (or tubulointerstitial fields) affected for statistical analysis. The percentage of glomeruli affected would determine focal versus diffuse disease processes but not necessarily segmental versus global glomerular lesions.

TEM. The digital TEM images from each case (9–26 images per case) were viewed and scored independently by the pathologists. The specific location of any glomerular electron-dense deposits and the remodeling of the glomerular basement membrane (GBM; as listed in Supplemental Table 3) were scored as absent (0), rare (1), or not rare (2). Additional TEM lesions were scored as absent (0) or present (1).

Table 1. Parameter Scores for Whole Renal Biopsy Evaluation by Light Microscopy.^a

Pattern of Injury	Control	FSGS		Amyloidosis	MPGN		MGN	
	Cluster 1	Cluster 2	Cluster 3	Cluster 4	Cluster 5	Cluster 6	Cluster 7	Cluster 8
Hypercellularity								
Endocapillary	0.0 (0.0–0.0)	0.3 (0.0–0.8)	0.5 (0.0–2.0)	0.0 (0.0–0.3)	3.0 (0.7–3.9)	2.4 (1.8–4.0)	0.7 ^b (0.0–2.8)	0.1 (0.0–1.0)
Mesangial	0.4 (0.4–0.7)	1.6 (0.8–2.0)	2.1 ^c (1.3–2.9)	0.6 (0.0–1.0)	2.8 (2.4–3.4)	2.6 (1.1–3.3)	2.0 ^c (1.1–3.0)	1.3 (0.3–1.9)
From neutrophils	0.0 (0.0–0.0)	0.0 (0.0–0.6)	0.3 ^b (0.0–0.8)	0.0 (0.0–0.6)	1.5 (0.1–2.8)	1.1 (0.0–2.8)	0.3 ^b (0.0–1.3)	0.0 (0.0–0.4)
Synechia	0.1 (0.0–0.7)	1.8 (0.8–2.0)	3.0 ^e (2.0–3.4)	1.2 (0.4–4.0)	3.0 ^e (2.3–4.0)	1.6 (0.6–2.8)	2.5 ^d (1.3–3.0)	1.1 (0.5–2.0)
Hyalinosis	0.0 (0.0–0.6)	1.0 (0.0–1.7)	2.0 ^d (0.3–3.4)	0.0 (0.0–0.3)	3.2 ^e (2.0–3.8)	0.8 (0.0–1.6)	1.0 ^b (0.3–2.0)	0.3 (0.0–1.3)
Capillary loop thickening	0.0 (0.0–0.1)	1.0 (0.3–1.8)	1.8 ^d (0.8–2.6)	0.8 (0.3–3.0)	2.9 (1.4–4.0)	2.5 (1.5–3.0)	3.0 ^e (2.3–3.8)	1.7 (1.1–2.3)
Immune deposits ^f	0.0 (0.0–0.0)	0.0 (0.0–0.4)	0.0 (0.0–0.1)	0.0 (0.0–0.0)	0.4 (0.0–1.9)	0.3 (0.0–2.4)	2.3 ^b (0.7–3.7)	1.6 (0.0–3.0)
GBM								
Spikes	0.0 (0.0–0.0)	0.0 (0.0–0.0)	0.0 (0.0–1.0)	0.0 (0.0–0.0)	0.0 (0.0–0.8)	0.3 (0.0–0.8)	2.4 ^d (2.0–3.8)	0.9 (0.1–2.4)
Holes	0.0 (0.0–0.0)	0.0 (0.0–0.3)	0.0 ^b (0.0–0.5)	0.0 (0.0–0.0)	0.0 (0.0–0.5)	0.3 (0.0–0.8)	1.8 ^d (0.3–2.8)	0.2 (0.0–1.0)
Amyloid	0.0 (0.0–0.0)	0.0 (0.0–0.0)	0.0 (0.0–0.0)	3.0 (1.9–4.0)	0.0 (0.0–0.0)	0.0 (0.0–0.0)	0.0 (0.0–0.0)	0.0 (0.0–0.0)
Mesangial matrix expansion	0.2 (0.0–0.5)	0.9 (0.4–3.0)	1.8 ^c (1.0–2.3)	2.8 (1.8–3.8)	2.7 (2.0–3.0)	2.0 (0.8–3.0)	1.1 (0.5–2.7)	0.8 (0.0–1.8)
Degree of sclerosis ^g	0.0 (0.0–0.0)	0.3 (0.0–1.4)	1.3 ^d (0.9–2.6)	0.0 (0.0–0.0)	1.2 (0.0–3.3)	0.5 (0.1–1.8)	0.6 ^c (0.0–2.1)	0.1 (0.0–0.9)
Interstitial								
Small arterial MHH ^h	0.0 (0.0–0.0)	0.3 (0.0–0.8)	0.8 ^c (0.1–1.0)	0.0 (0.0–0.5)	0.5 (0.0–1.0)	0.6 (0.0–1.0)	0.5 ^b (0.0–1.0)	0.0 (0.0–0.6)
Fibrosis ⁱ	0.0 (0.0–0.0)	0.5 (0.0–1.6)	0.5 (0.2–1.7)	0.3 (0.0–1.4)	0.8 (0.1–1.7)	0.3 (0.1–0.9)	0.4 ^b (0.0–1.2)	0.1 (0.0–0.4)
Inflammation ⁱ	0.0 (0.0–0.3)	0.4 (0.0–1.2)	0.8 ^b (0.2–1.8)	0.2 (0.0–0.9)	1.0 ^c (0.6–1.4)	0.5 (0.3–1.3)	0.6 (0.0–1.4)	0.3 (0.0–1.0)

Abbreviations: FSGS, focal segmental glomerulosclerosis; GBM, glomerular basement membrane; MGN, membranous glomerulonephropathy; MHH, medial hypertrophy/hyperplasia; MPGN, membranoproliferative glomerulonephritis.

^aValues are presented as medians (minimum–maximum) and based on scores ranging from 0 to 4, with exceptions noted. All parameters listed were part of the 59-parameter data set. *P* value comparisons made between clusters 2 and 3, clusters 5 and 6, or clusters 7 and 8.

^b*P* < 0.05.

^c*P* < 0.01.

^d*P* < 0.001.

^e*P* < 0.0001.

^fFuchsinophilic deposits with Masson trichrome staining.

^gCriteria based on distribution of sclerosis in the glomerular tuft: 0, no sclerosis; 1, <25% involvement; 2, 25%–50%; 3, 51%–75%; 4, >75%.

^hValues based on a scale of 0 (absent) or 1 (present).

ⁱValues represented the character of interstitial fibrosis or inflammation—no fibrosis/inflammation, no distortion of architecture by fibrosis/inflammation, separation of tubules by fibrosis/inflammation, and replacement of tubules by fibrosis/inflammation—and were graded on scale of 0–3.

IF. Diagnostic evaluation of IF labeling patterns (Supplemental Table 3) was performed by G.E.L. and J.J.v.d.L., and representative digital photographs of 1 to 3 glomeruli with notable labeling with each antibody were taken at that time. All pathologists evaluated the IF images for each case prior to group discussions, and by consensus agreement, the scores used in the data analysis for the IgG, IgM, IgA, and C3 immunostains were those provided by 1 pathologist (R.E.C.) who had extensive training and experience evaluating glomerular IF labeling patterns. Specifically, a score of 2 was given when there was

consistent granular labeling in the mesangium or capillary walls above the background autofluorescence of the tubulointerstitial compartment. A stain was deemed equivocal and given a score of 1 when there were a few scattered granules or labeling of low intensity in the glomeruli. Nonspecific labeling patterns (eg, not granular) and the absence of positive labeling were scored as 0.

Statistical Analysis. Hierarchical cluster analysis was used to organize the cases into groups. Within each group (cluster),

Table 2. Parameter Scores for Individual Glomeruli and Tubulointerstitial Fields by Light Microscopy.^a

Pattern of Injury	Control	FSGS		Amyloidosis	MPGN		MGN	
	Cluster 1	Cluster 2	Cluster 3	Cluster 4	Cluster 5	Cluster 6	Cluster 7	Cluster 8
GBM hyalinosis	2 (0–7)	11 (0–28)	21 (0–66)	5 (0–14)	63 ^d (27–95)	17 (0–41)	19 ^b (0–63)	3 (0–19)
Synechiae	6 (0–14)	28 (14–65)	60 ^b (39–86)	42 (13–100)	73 ^b (50–86)	51 (12–76)	43 ^b (9–75)	26 (16–50)
Percentage of glomeruli with:								
Mesangial matrix expansion	25 (0–45)	63 (28–100)	82 ^d (55–94)	97 (79–100)	95 (85–100)	85 (50–100)	74 (31–100)	50 (0–93)
Glomerulosclerosis	0 (0–0)	28 (3–60)	72 ^d (47–100)	0 (0–0)	61 (0–100)	35 (3–75)	33 ^b (0–95)	9 (0–58)
Obsolescent glomeruli	0 (0–0)	7 (0–33)	22 ^b (0–43)	4 (0–25)	7 (0–38)	2 (0–13)	8 (0–28)	2 (0–12)
Nuclear debris	1 (0–4)	8 (0–25)	20 ^b (0–42)	24 (5–75)	43 (19–73)	36 (0–73)	21 (0–69)	10 (0–36)
Periglomerular Inflammation	3 (0–11)	8 (0–30)	30 ^b (3–75)	15 (0–39)	43 (15–82)	27 (0–72)	22 (0–55)	17 (0–74)
Fibrosis	3 (0–7)	12 (0–33)	19 (0–50)	11 (0–50)	51 ^b (15–86)	18 (0–50)	14 (0–56)	4 (0–15)
Parietal cell Hypertrophy	6 (0–14)	27 (9–58)	36 (19–60)	24 (9–63)	60 (21–85)	46 (13–75)	34 (10–58)	33 (14–56)
Hyperplasia	4 (0–14)	14 (0–44)	24 (6–58)	18 (0–75)	44 ^b (25–62)	27 (12–50)	21 (10–34)	18 (0–50)
Glomerular inflammatory cells	3 (0–7)	7 (0–27)	9 (0–25)	10 (0–33)	42 (8–73)	39 (0–91)	12 (0–50)	12 (0–29)
GBM duplication	3 (0–11)	7 (0–37)	12 (0–43)	6 (0–38)	40 (13–58)	45 (9–82)	20 (0–67)	20 (0–75)
Bowman capsule BM splitting	10 (0–18)	15 (0–43)	20 (6–38)	7 (0–25)	40 ^d (0–75)	13 (0–28)	17 ^d (0–63)	4 (0–15)
Tubular Epithelial single-cell necrosis	1 (0–4)	22 (0–67)	34 (9–58)	32 (8–67)	44 (17–71)	33 (5–67)	23 (0–50)	18 (0–61)
Regeneration	2 (0–7)	11 (0–35)	12 (0–30)	15 (0–33)	26 (0–57)	18 (0–44)	11 (0–39)	11 (0–21)
EC pigment	19 (4–50)	27 (0–73)	38 (7–79)	30 (8–96)	26 (0–63)	50 (4–100)	37 (4–75)	35 (0–81)
EC isometric vesiculation	9 (0–21)	7 (0–33)	7 (0–20)	11 (0–93)	8 (0–33)	6 (0–32)	4 (0–14)	18 ^d (0–42)
Arteriolar hyalinosis ^e	0 (0–0)	11 (0–67)	16 (0–47)	1 (0–7)	34 ^b (0–75)	7 (0–33)	6 (0–43)	5 (0–20)
Interstitial Fibrosis ^f	0 (0–0)	9 (0–34)	8 (1–25)	6 (0–31)	11 ^b (1–35)	2 (0–4)	5 ^d (0–28)	1 (0–3)
Inflammation ^f	0 (0–1)	3 (0–9)	9 ^d (1–20)	3 (0–12)	7 ^d (3–11)	3 (1–6)	3 (0–7)	2 (0–10)

Abbreviations: BM, basement membrane; EC, epithelial cell; FSGS, focal segmental glomerulosclerosis; GBM, glomerular basement membrane; MGN, membranous glomerulonephropathy; MPGN, membranoproliferative glomerulonephritis.

Values presented as mean percentages (minimum–maximum) and based on scoring a range of 4 to 32 glomeruli. All parameters listed were part of the 59-parameter data set. *P* value comparisons made between clusters 2 and 3, clusters 5 and 6, or clusters 7 and 8.

^b*P* < 0.05.

^c*P* < 0.01.

^d*P* < 0.001.

^eBoth afferent and efferent arterioles.

^fInterstitial fibrosis and inflammation based on percentage of fields affected.

cases had greater similarity to one another (in terms of the evaluated lesions) than they did to cases from other groups. Cluster analysis therefore objectively organized the cases into distinct

groups of dogs having similar pathologic changes (patterns of injury). The procedure used for this analysis was Ward's linkage with L2 dissimilarity (Stata/IC 12 for Windows, StataCorp

Table 3. Parameter Scores for Electron-Dense Deposit Location and GBM Remodeling Evaluated by Transmission Electron Microscopy.^a

Pattern of Injury	Control	FSGS		Amyloidosis	MPGN		MGN	
	Cluster 1	Cluster 2	Cluster 3	Cluster 4	Cluster 5	Cluster 6	Cluster 7	Cluster 8
Electron-dense deposits								
Subepithelial	0.0 (0.0–0.0)	0.0 (0.0–0.0)	0.0 (0.0–0.0)	0.0 (0.0–0.0)	0.0 (0.0–2.0)	2.0 ^b (0.0–2.0)	2.0 (1.0–2.0)	2.0 (2.0–2.0)
Subendothelial	0.0 (0.0–0.0)	0.0 (0.0–2.0)	0.0 (0.0–0.0)	0.0 (0.0–0.0)	2.0 (2.0–2.0)	2.0 (2.0–2.0)	0.0 (0.0–2.0)	0.0 (0.0–2.0)
Mesangial	0.0 (0.0–0.0)	0.0 (0.0–2.0)	0.0 (0.0–2.0)	0.0 (0.0–0.0)	2.0 (0.0–2.0)	2.0 ^b (2.0–2.0)	2.0 (0.0–2.0)	0.5 (0.0–2.0)
Paramesangial	0.0 (0.0–0.0)	0.0 (0.0–0.0)	0.0 (0.0–0.0)	0.0 (0.0–0.0)	0.0 (0.0–2.0)	2.0 ^b (0.0–2.0)	2.0 (1.0–2.0)	2.0 (1.0–2.0)
Intramembranous	0.0 (0.0–0.0)	0.0 (0.0–0.0)	0.0 (0.0–1.0)	0.0 (0.0–0.0)	1.0 (0.0–2.0)	1.0 (0.0–2.0)	2.0 ^b (1.0–2.0)	1.0 (0.0–2.0)
Encircled	0.0 (0.0–0.0)	0.0 (0.0–0.0)	0.0 (0.0–0.0)	0.0 (0.0–0.0)	0.0 (0.0–1.0)	0.0 (0.0–2.0)	2.0 ^b (1.0–2.0)	1.0 (0.0–2.0)
GBM spikes	0.0 (0.0–0.0)	0.0 (0.0–0.0)	0.0 (0.0–0.0)	0.0 (0.0–0.0)	0.0 (0.0–0.0)	1.0 ^c (0.0–2.0)	2.0 ^b (1.0–2.0)	1.0 (0.0–2.0)

Abbreviations: FSGS, focal segmental glomerulosclerosis; GBM, glomerular basement membrane; MGN, membranous glomerulonephropathy; MPGN, membranoproliferative glomerulonephritis.

^aValues presented as medians (minimum–maximum) and based on scores ranging from 0 to 2: 0, absent; 1, rare; 2, not rare. All parameters listed were part of the 59-parameter data set. *P* value comparisons made between clusters 2 and 3, clusters 5 and 6, or clusters 7 and 8.

^b*P* < .05.

^c*P* < .01.

LP, College Station, TX, USA). Results of each analysis were displayed as a dendrogram in which the shorter the vertical lines under the horizontal bar connecting 2 animals (or groups of animals), the lesser the dissimilarity among shared parameters.

Cluster analysis was performed on 3 data sets containing the same number of cases but differing in the number of lesions (parameters) evaluated. The first data set contained all 114 parameters (LM, *n* = 76; TEM, *n* = 30; IF, *n* = 8). The second, which had 59 parameters (LM, *n* = 35; TEM, *n* = 16; IF, *n* = 8), was a limited list selected by the pathologists, based on their expertise gained during the course of the study. This limited list excluded parameters that were rarely observed or deemed to be uninformative. Last, the third dendrogram was generated from the 59-parameter data set using only LM lesions (35 parameters).

Some of the categorical values for IF were missing because the biopsy tissue apportioned for IF did not contain glomeruli for some or all of the immunostains. This included cases of glomerular amyloidosis (5 cases), membranous glomerulonephropathy (MGN; 3 cases), and glomerulosclerosis (1 case). Because cluster analysis cannot be performed on data sets with missing values, a method was developed to add imputed values for the missing data. Ordinal logistic regression was used to predict the probability of an individual with missing data falling into 1 of the 3 possible mutually exclusive categories (0, 1, 2) as a function of other variables believed a priori to be associated with IF. The category with the highest predicted probability was assigned for each individual's missing IF value.

Based on the 59-parameter data set, Mann-Whitney tests were performed with the same software to determine if significant differences existed for the parameters within clusters

exhibiting similar glomerular disease patterns (cluster 2 vs cluster 3, cluster 5 vs cluster 6, and cluster 7 vs cluster 8).

Results

Cluster Analysis

Ninety-six dogs (including the 5 controls) were scored and a preliminary cluster analysis performed (data not shown). This preliminary cohort contained 7 cases with rare diagnoses—including 1 collagenofibrotic glomerulonephropathy (based on the presence of type III collagen within the capillary wall and mesangium), 1 canine Alport syndrome (based on the lack of normal type IV collagen in the GBM), 2 nonamyloidotic fibrillary glomerulonephropathies, 1 podocytopathy, and 2 cases with GBM defects of undetermined pathogenesis. Given that these cases obscured the findings of the patterns of the larger clusters, the decision was made to remove them from the cohort so that the study could focus on the patterns of common types of canine glomerular disease. Exclusion of these 7 cases resulted in a cohort of 5 controls (from the Texas Veterinary Renal Pathology Service center) and 84 proteinuric dogs (73 from the Texas Veterinary Renal Pathology Service center and 11 from the Utrecht Veterinary Nephropathology Service center). Fifty-nine cases had been prospectively enrolled through the WSAVA-sponsored study, and the remaining cases were routine diagnostic samples that met the aforementioned criteria. Needle core biopsies were performed in 72 dogs; 16 dogs had surgical wedge biopsies; and 1 dog had a surgical punch biopsy.

The dendrogram generated from the 114-parameter set had 2 large branches (Fig. 1). The cases on the right (*n* = 46) were

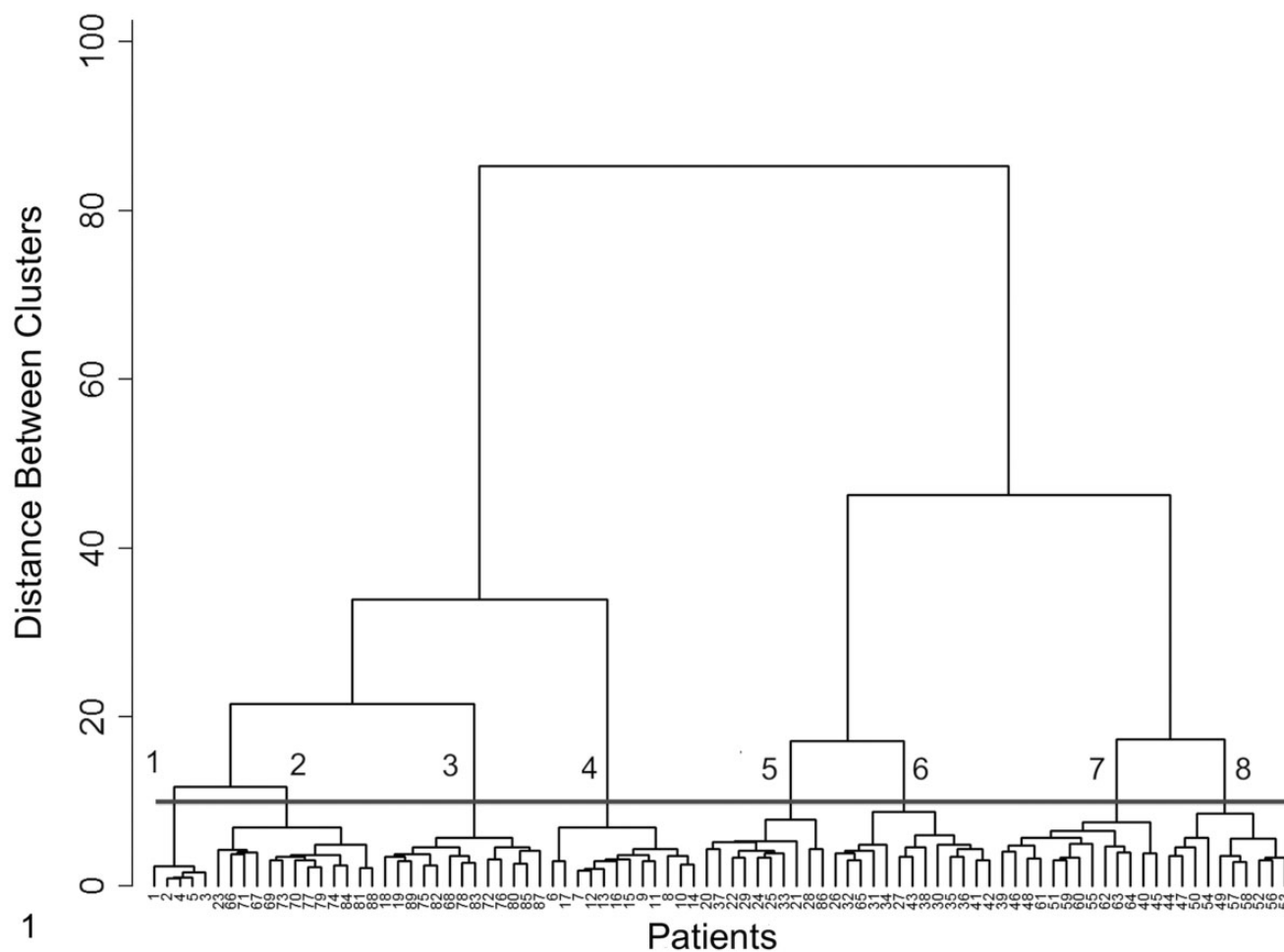


Figure 1. Dendrogram of 89 patients based on cluster analysis evaluation of 114 parameters related to all compartments of the kidney. Evaluation was performed by light microscopy, transmission electron microscopy, and immunofluorescence microscopy. The numbered (1–8) horizontal bar shows the level of discrimination that delineates the 8 clusters identified. Cluster 1 was composed of 5 control animals with normal glomerular morphology, clinical findings, and laboratory values. Clusters 2 and 3 comprised cases with glomerulosclerosis. Interestingly, cases in cluster 2 shared more similarities to controls in cluster 1 than to cases in cluster 3, as demonstrated by the presence of a connecting link between clusters 1 and 2. Cluster 4 comprised cases of glomerular amyloidosis. Cases in clusters 5 and 6 and clusters 7 and 8 had patterns that were characteristic of membranoproliferative glomerulonephritis and membranous glomerulonephropathy, respectively.

defined by the presence of electron-dense (immune complex) deposits and were considered to have immune complex-mediated glomerulonephritis (ICGN), whereas cases on the left ($n = 43$, including the 5 controls) did not typically have immune deposits and were considered to be non-ICGN. Of note, there were 7 cases in the non-ICGN branch with equivocal evidence that immune complexes might have played a role in the evolution of their glomerular disease; however, the dominant phenotype at the time of biopsy was that of glomerulosclerosis. These exceptions are discussed below in the glomerulosclerosis section. The 2 large branches disaggregated into progressively smaller groups and eventually partitioned into 8 distinct clusters (Fig. 1). Cluster 1 was composed of the 5 control animals with normal glomerular morphology, clinical findings, and laboratory values. Clusters 2 and 3 comprised cases with glomerulosclerosis. Interestingly, cases in cluster

2 shared more similarities to controls in cluster 1 than to cases in cluster 3, as demonstrated by the presence of a connecting link between clusters 1 and 2. Cluster 4 comprised cases of glomerular amyloidosis. Cases in clusters 5 and 6 and clusters 7 and 8 had patterns that were characteristic of membranoproliferative glomerulonephritis (MPGN) and MGN, respectively.

A dendrogram of the 59-parameter data set was also generated (Fig. 2). Similar to the 114-parameter data set, this dendrogram clearly showed a division of cases into 8 distinct clusters. With 1 exception, the case composition of each cluster was identical to the case composition of the clusters formed from the larger, 114-parameter data set. However, the ordering of cases and the formation of smaller subclusters differed between the 2 dendrograms, and 1 case moved from cluster 6 to cluster 7, representing a shift from a MPGN pattern to a MGN pattern.

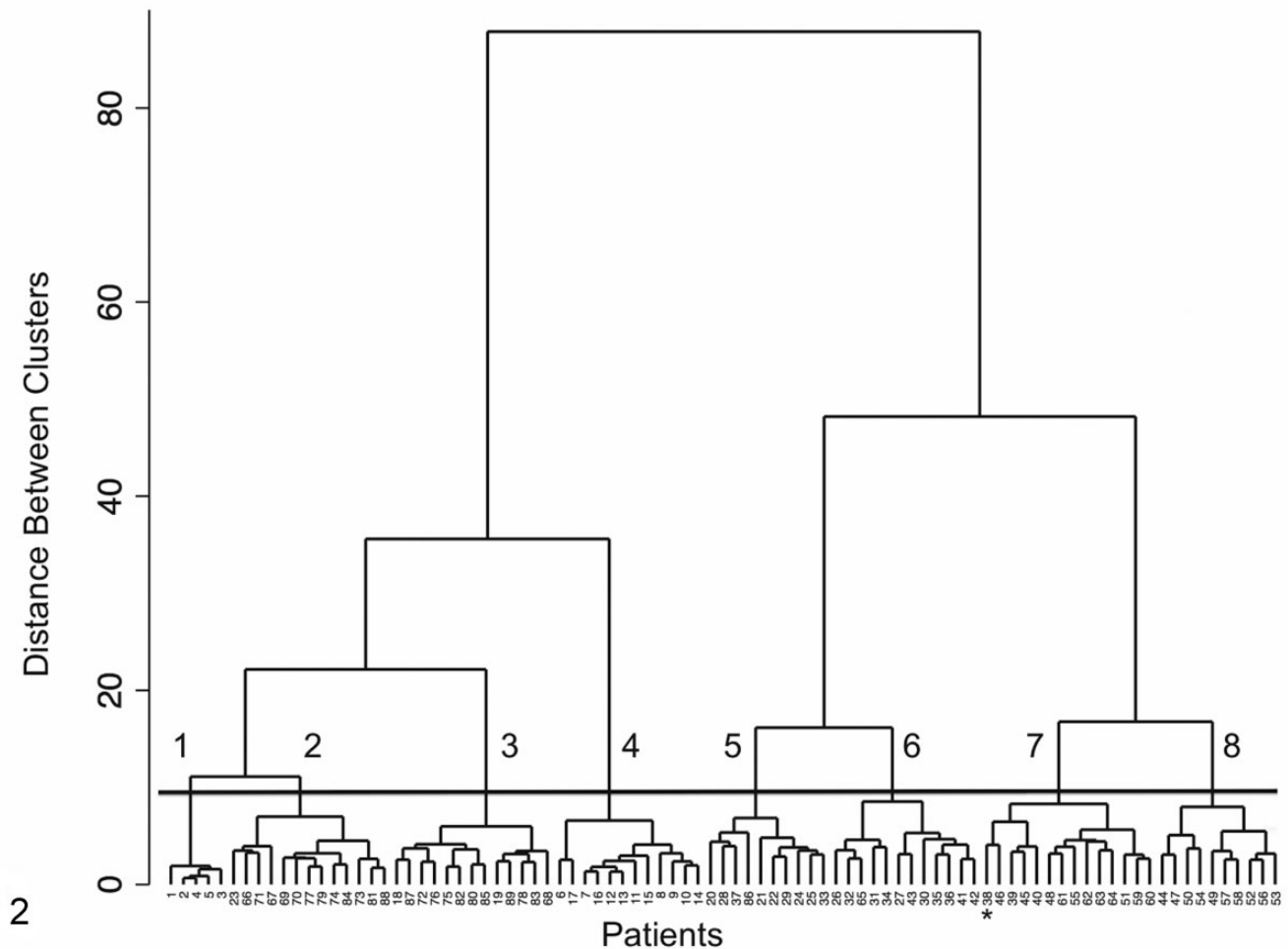


Figure 2. Dendrogram of 89 patients based on cluster analysis of 59 parameters related to all compartments of the kidney and evaluated by light microscopy, transmission electron microscopy, and immunofluorescence microscopy. The numbered (1–8) horizontal bar shows the level of discrimination that delineates the 8 clusters identified. The star indicates a case that moved from cluster 6 in the 114-parameter dendrogram to cluster 7 in the 59-parameter dendrogram.

Often the only modality routinely available for evaluation of renal tissue is LM; therefore, cluster analysis was also performed on only the LM lesions (31 parameters) from the 59-parameter data set (Fig. 3). This enabled comparison of the LM-only dendrogram to Figure 2. While the LM-only dendrogram also contained 8 clusters, it failed to correctly distinguish a number of ICGN cases from non-ICGN cases. Specifically, 8 of the MGN cases (7 of 10 cases in cluster 8 and 1 of 14 cases in cluster 7)—all of which had unequivocal evidence of immune deposits demonstrated with TEM and IF—moved to the non-ICGN side of the dendrogram. In addition, all 13 cases in cluster 3 and 1 of 13 cases in cluster 2 (glomerulosclerosis clusters) moved to the ICGN side of the dendrogram.

Control Kidneys

Five controls had glomeruli with minimal lesions via all analyses of renal biopsies and were considered normal (cluster 1). All 5 dogs were initially enrolled into the study as controls

because they lacked proteinuria and azotemia. Most glomeruli were histologically normal. Specifically, glomerular tufts were usually normocellular; capillary walls were thin; and the mesangium was not expanded (Figs. 4–7). Fuchsinophilic deposits were not observed with TRI stain (Fig. 6). Minimal histologic lesions were identified in a few glomeruli from each biopsy, including mild segmental mesangial cell hypercellularity (≥ 3 mesangial cell nuclei in close apposition) and mild mesangial expansion. Notably, segmental glomerulosclerosis was not present (Tables 1 and 2). Small synechiae and GBM hyalinosis were rarely observed (Tables 1 and 2).

Ultrastructurally, podocyte foot processes were largely intact, and the GBM was uniform and homogeneous (Fig. 8). Electron-dense deposits or fibrils were not present (Tables 3 and 4). Cellular interpositioning, GBM rarefaction, and GBM wrinkling were rarely observed in control dogs. IF revealed unequivocal granular IgM labeling in the mesangium in 2 cases (Fig. 9); 1 of these cases also had IgM labeling within the capillary walls. Unequivocal labeling for other immunoreactants

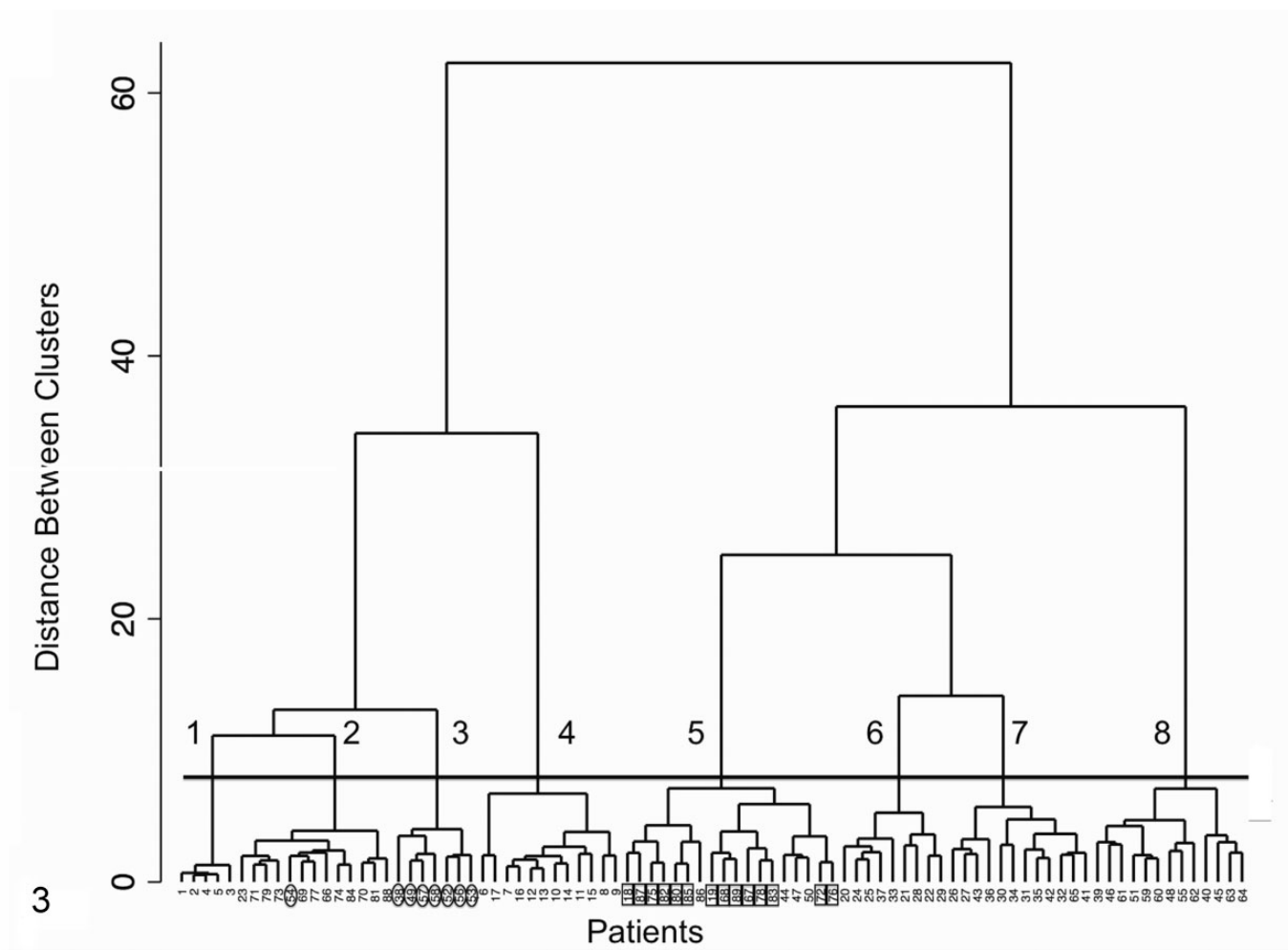


Figure 3. Evaluation of 35 light microscopic parameters derived from the 59-parameter data set. The numbered (1–8) horizontal bar shows the level of discrimination that delineates the 8 clusters identified. Ovals indicate cases that moved from clusters 7 and 8 of the 59-parameter data set (represented by Fig. 2) to clusters 2 and 3 of the 35-parameter data set. Rectangles indicate cases that moved from clusters 2 and 3 of the 59-parameter data set to cluster 5 of the 35-parameter data set.

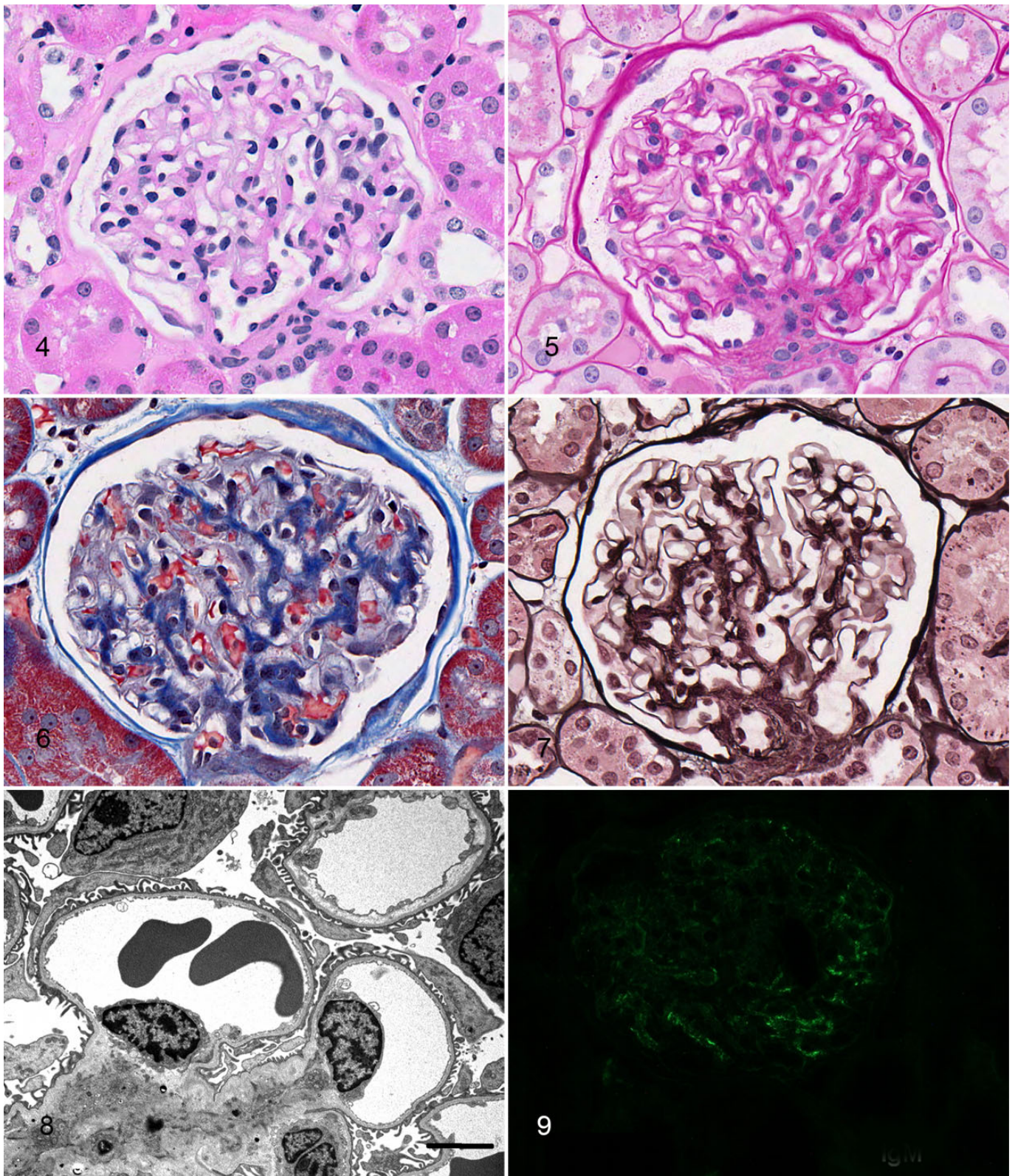
was not identified in the mesangium or capillary walls (Table 5). Because electron-dense deposits were not identified ultrastructurally, the IgM labeling was considered nonspecific.

Control dogs were not proteinuric, azotemic, or hypoalbuminemic (Table 6). However, 4 of the 5 dogs had systolic blood pressures between 160 and 180 mm Hg and the fifth dog, 146mm Hg. The Greyhound breed has been reported to have higher blood pressure than that of other breeds; this elevation in systolic blood pressure has been attributed to the white-coat effect.²⁸ Interestingly, the dog with the highest reading (176 mm Hg) had the highest percentage of glomeruli with synechiae and hyalinosis (data not shown).

Focal Segmental Glomerulosclerosis

Of 89 cases, 26 (29%) grouped into cluster 2 (13 cases) and cluster 3 (13 cases); all had lesions characteristic of the pattern of focal segmental glomerulosclerosis (FSGS). The defining LM lesion of these clusters was solidification of a

portion of the capillary tuft in at least 1 glomerulus. This segmental solidification was attributed to mesangial matrix expansion and effacement of the capillary lumen, often in association with some degree of mesangial hypercellularity (Figs. 10–13). The distribution of the sclerosis within the glomerular tuft (hilar, near the origin of the proximal tubule, or not at either of the poles) was highly variable among the glomeruli, even within a single biopsy core. Glomerulosclerosis was more severe and affected more glomeruli in cluster 3 compared with cluster 2 (Tables 1 and 2). Specifically, the percentage of nonobsolescent glomeruli affected by FSGS ranged from 3% to 100%, with a significantly higher percentage of affected glomeruli in cluster 3 compared with cluster 2. Synechiae and hyalinosis of the tuft were commonly observed lesions in FSGS and were likewise more extensive in cluster 3 compared with cluster 2 (Tables 1 and 2). A significantly higher percentage of glomeruli in cluster 3 had synechiae, mesangial matrix expansion, nuclear debris, and periglomerular inflammation when compared with glomeruli in cluster



Figures 4–9. Normal glomerulus, control dog, cluster I. **Figures 4–7.** The glomerulus is normocellular; mesangium is not expanded; and the glomerular basement membrane is of normal thickness with a smooth outer contour. There is mild thickening and splitting of the basement membrane of Bowman capsule. **Figure 4.** Hematoxylin and eosin. **Figure 5.** Periodic acid–Schiff reaction. **Figure 6.** Masson trichrome. **Figure 7.** Jones methenamine silver. **Figure 8.** Normal glomerular capillary loops from the same dog. Capillary lumens are open, and endothelial cells are at the base of the capillary loops. Podocyte foot processes are perpendicularly oriented along the capillary walls. One capillary loop in upper-right corner has subendothelial widening. Bar = 2 μ m. Transmission electron microscopy. **Figure 9.** Immunofluorescence for IgM shows scattered, equivocal staining at the periphery of the tuft.

Table 4. Parameter Scores for Glomeruli Evaluated by Transmission Electron Microscopy.^a

Pattern of Injury	Control	FSGS		Amyloidosis	MPGN		MGN	
	Cluster 1	Cluster 2	Cluster 3	Cluster 4	Cluster 5	Cluster 6	Cluster 7	Cluster 8
Mesangial cell interpositioning	0.43 (0.00–0.43)	0.75 (0.00–1.00)	0.86 (0.25–1.00)	0.00 (0.00–0.50)	1.00 (0.88–1.00)	1.00 (0.75–1.00)	0.75 (0.25–1.00)	0.63 (0.00–1.00)
Endothelial cell swelling	0.00 (0.00–0.00)	0.00 (0.00–0.50)	0.00 (0.00–0.25)	0.00 (0.00–0.14)	0.50 (0.29–1.00)	0.29 (0.13–0.75)	0.00 (0.00–0.50)	0.00 (0.00–0.83)
Diffuse GBM thickening	0.00 (0.00–0.00)	0.00 (0.00–0.75)	0.25 ^b (0.00–1.00)	0.00 (0.00–1.00)	0.00 (0.00–0.43)	0.13 (0.00–0.57)	0.25 ^b (0.00–0.75)	0.00 (0.00–0.43)
Intravascular inflammatory cells	0.00 (0.00–0.14)	0.00 (0.00–0.50)	0.00 (0.00–0.50)	0.00 (0.00–0.38)	0.25 (0.00–0.71)	0.25 (0.00–0.75)	0.00 (0.00–0.25)	0.06 (0.00–0.14)
GBM								
Rarefaction	0.29 (0.14–0.43)	0.38 (0.00–0.75)	0.50 (0.00–0.75)	0.07 (0.00–0.50)	0.20 (0.00–0.67)	0.13 (0.00–0.50)	0.25 (0.00–0.57)	0.13 (0.00–0.57)
Wrinkling	0.43 (0.00–0.71)	0.43 (0.00–0.88)	0.50 (0.00–1.00)	0.15 (0.00–0.75)	0.43 (0.13–1.00)	0.25 (0.00–0.50)	0.25 (0.00–0.60)	0.13 (0.00–0.38)
Podocyte microvillus transformation	0.00 (0.00–0.00)	0.25 (0.00–1.00)	0.50 (0.00–0.86)	0.25 (0.00–1.00)	0.50 (0.00–0.71)	0.50 (0.00–0.88)	0.75 (0.00–1.00)	0.80 (0.38–1.00)
Endothelial cell cytoplasmic vacuoles	0.00 (0.00–0.00)	0.00 (0.00–0.75)	0.25 (0.00–0.75)	0.00 (0.00–0.25)	0.21 (0.00–0.80)	0.25 (0.00–0.43)	0.00 (0.00–0.25)	0.13 (0.00–0.33)
Amyloid fibrils	0.00 (0.00–0.00)	0.00 (0.00–0.00)	0.00 (0.00–0.13)	1.00 (1.00–1.00)	0.00 (0.00–0.00)	0.00 (0.00–0.00)	0.00 (0.00–0.00)	0.00 (0.00–0.00)

Abbreviations: FSGS, focal segmental glomerulosclerosis; GBM, glomerular basement membrane; MGN, membranous glomerulonephropathy; MPGN, membranoproliferative glomerulonephritis.

^aValues presented as median scores (minimum–maximum) and based on scores ranging from 0 (absent) to 1 (present). All parameters listed were part of the 59-parameter data set.

^b*P* < .05. *P* value comparisons made between clusters 2 and 3, clusters 5 and 6, or clusters 7 and 8.

2. In 19 of the 26 cases composing clusters 2 and 3, obsolescent glomeruli were present, involving 0% to 43% of the total number of glomeruli in the biopsies. Obsolescent glomeruli were significantly more prevalent in cluster 3 than in cluster 2. Although not tested for significance, the mean percentage of obsolescent glomeruli in cluster 3 was 22%, whereas it ranged from 0% to 8% in the other clusters. Capillary wall thickening was often mild in cluster 2 but mild to moderate in cluster 3 (Table 1). Seven of 13 cases in cluster 3 and 1 of 13 cases in cluster 2 had rare changes in the GBM, interpreted via LM to be spike or hole formation; however, none of these cases had evidence of GBM spikes or holes ultrastructurally. Of 26 cases in clusters 2 and 3, 3 (12%) exhibited segmental distortion of glomerular tufts due to the presence of lipid-laden macrophages (glomerular lipodosis). This lesion was not present in control dogs or in any other disease category in this study.

The percentages of tubulointerstitial fields with fibrosis and the severity of the fibrosis were not significantly different between clusters 2 and 3. The percentages of fields affected by inflammation and the severity of inflammation were significantly greater in cluster 3 compared with cluster 2.

Although TEM (Fig. 14) revealed extensive foot process effacement in FSGS, this lesion was not specific for clusters 2 and 3, because it was identified in all proteinuric dogs. Common ultrastructural lesions included wrinkling of the GBM, GBM rarefaction, mesangial cell interpositioning, microvillus transformation of podocytes, and (in cluster 3)

diffuse GBM thickening (Table 4). Electron-dense deposits were not present in 19 cases. However, 4 cases from cluster 2 and 2 cases from cluster 3 contained mesangial electron-dense deposits by TEM. Two of these cases also had subendothelial electron-dense deposits, which were rare in 1 case and not rare in the other. One additional case had rare intramembranous electron-dense deposits only. Other TEM and LM lesions in these 7 cases with demonstrable electron-dense deposits were similar to those present in FSGS cases without deposits.

IF (Fig. 15) revealed positive capillary wall and/or mesangial labeling of varying intensity for various immunoreactants in many of the FSGS cases and did not distinguish between cases with and without electron-dense deposits. Eight cases had negative or equivocal IF staining patterns. Eleven cases had unequivocally positive IF labeling but no ultrastructural evidence of electron-dense deposits. Of the 7 cases with electron-dense deposits noted on TEM, only 4 had granular IgM mesangial staining. One of these 4 also had granular IgG staining along capillary walls, whereas another had granular C3 staining within the mesangium and along capillary walls.

As a group, dogs in cluster 3 had slightly higher median UPC and SCr values and a greater frequency of hypertension when compared with dogs in cluster 2 (Table 6), suggesting a trend toward more severe clinical manifestations of disease for dogs in cluster 3 versus those in cluster 2. However, the differences were small, and the variation among dogs in each cluster

Table 5. Parameter Scores for Glomeruli Evaluated by Immunofluorescence Microscopy.^a

Pattern of Injury	Control	FSGS		Amyloidosis	MPGN		MGN	
	Cluster 1	Cluster 2	Cluster 3	Cluster 4	Cluster 5	Cluster 6	Cluster 7	Cluster 8
IgG								
Mesangium	0.0 (0.0–1.0)	1.0 (0.0–2.0)	0.0 (0.0–1.0)	0.0 (0.0–1.0)	1.0 (0.0–2.0)	2.0 (0.0–2.0)	1.0 (0.0–2.0)	0.5 (0.0–2.0)
Capillary wall	0.0 (0.0–0.0)	0.0 (0.0–2.0)	0.0 (0.0–1.0)	0.0 (0.0–1.0)	2.0 (0.0–2.0)	2.0 (1.0–2.0)	2.0 (1.0–2.0)	2.0 (1.0–2.0)
IgM								
Mesangium	1.0 (1.0–2.0)	2.0 (0.0–2.0)	1.0 (0.0–2.0)	0.0 (0.0–2.0)	2.0 (0.0–2.0)	2.0 (0.0–2.0)	1.0 (0.0–2.0)	1.5 (0.0–2.0)
Capillary wall	0.0 (0.0–2.0)	1.0 ^b (0.0–2.0)	0.0 (0.0–1.0)	0.0 (0.0–1.0)	1.5 (0.0–2.0)	2.0 (0.0–2.0)	1.0 (0.0–2.0)	1.5 (0.0–2.0)
IgA								
Mesangium	0.0 (0.0–0.0)	0.0 (0.0–2.0)	0.0 (0.0–1.0)	0.0 (0.0–1.0)	0.0 (0.0–1.0)	0.0 (0.0–1.0)	0.0 (0.0–2.0)	0.0 (0.0–2.0)
Capillary wall	0.0 (0.0–0.0)	0.0 (0.0–2.0)	0.0 (0.0–1.0)	0.0 (0.0–1.0)	0.0 (0.0–1.0)	0.0 (0.0–1.0)	0.0 (0.0–2.0)	0.0 (0.0–2.0)
C3								
Mesangium	0.0 (0.0–1.0)	0.0 (0.0–2.0)	0.0 (0.0–2.0)	0.0 (0.0–2.0)	2.0 (0.0–2.0)	2.0 (0.0–2.0)	2.0 (0.0–2.0)	1.0 (0.0–2.0)
Capillary wall	0.0 (0.0–0.0)	0.0 (0.0–2.0)	0.0 (0.0–2.0)	0.0 (0.0–1.0)	2.0 (0.0–2.0)	2.0 (1.0–2.0)	2.0 (1.0–2.0)	2.0 (0.0–2.0)

Abbreviations: FSGS, focal segmental glomerulosclerosis; MGN, membranous glomerulonephropathy; MPGN, membranoproliferative glomerulonephritis.

^aValues presented as median scores (minimum–maximum) and based on the absence or presence of a fluorescent granular pattern ranging from 0 to 2: 0, absent; 1, equivocal; 2, present. All parameters listed were part of the 59-parameter data set.

^b*P* < .05. *P* value comparisons made between clusters 2 and 3, clusters 5 and 6, or clusters 7 and 8.

Table 6. Clinical Data.

Clinical Variable	Control ^a	FSGS		Amyloidosis	MPGN		MGN	
	Cluster 1 <i>n</i> = 5	Cluster 2 <i>n</i> = 13	Cluster 3 <i>n</i> = 13	Cluster 4 <i>n</i> = 12	Cluster 5 <i>n</i> = 10	Cluster 6 <i>n</i> = 13	Cluster 7 <i>n</i> = 13	Cluster 8 <i>n</i> = 10
UPC								
Median	0.13	5.6	8.7	9.8	16.1	9.6	8.9	16.0
Min–Max	0.05–0.25	2.6–26.3	5.1–24.5	6.2–26.1	6.9–23.6	3.7–30.1	3.4–21.9	4.2–42.7
SCr, mg/dl								
Median	1.6	1.1	1.3	1.2	3.6	1.6	1.1	1.0
Min–Max	1.1–1.8	0.5–4.8	0.5–4.2	0.6–8.6	1.0–5.7	0.7–3.6	0.8–3.7	0.6–4.2
SAlb, g/dl								
Median	3.8	2.3	2.4	1.8	1.4	1.6	1.6	1.6
Min–Max	3.6–4.4	1.3–3.8	1.5–4.1	0.9–2.4	1.0–1.9	1.1–3.1	1.1–3.1	0.7–2.7
Hypertension, ^b <i>n</i>	4 of 5	5 of 13	9 of 13	3 of 11	9 of 10	10 of 12	4 of 10	6 of 8

Abbreviations: FSGS, focal segmental glomerulosclerosis; MGN, membranous glomerulonephropathy; MPGN, membranoproliferative glomerulonephritis; SAlb, serum albumin concentration (reference interval, 2.5–4.0 g/dl); SCr, serum creatinine concentration (reference interval, 0.5–1.5 mg/dl); UPC, urine protein:creatinine ratio (reference interval, <0.5).

^aAll control dogs were female greyhounds.

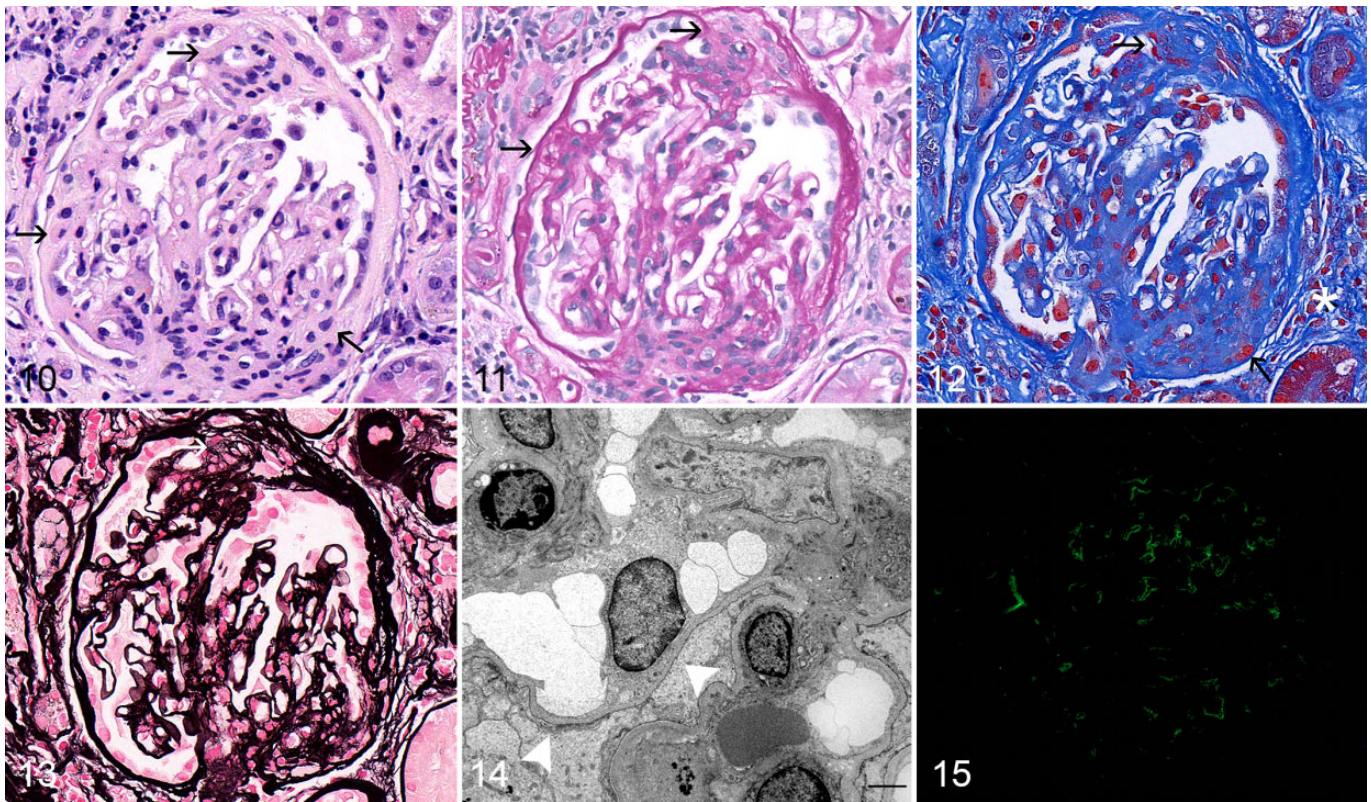
^bHypertension as defined in the text.

was large; therefore, statistically significant differences were not identified.

Amyloid

Of 89 cases, 12 (13%) grouped into cluster 4, and all were diagnosed with glomerular amyloidosis. The defining LM feature

of this cluster was expansion of the mesangium and compression of peripheral capillary loops by congophilic material that was birefringent under polarized light. Amyloid was present as scattered small nodules in 3 of the cases and as larger, easily discernible, coalescing to occasionally global deposits in the remaining cases (Fig. 16–21). Amyloid was pink and waxy when stained with PAS, was mottled blue to orange with TRI,



Figures 10–15. Focal segmental glomerulosclerosis, dog, cluster 3. **Figures 10–13.** There is segmental consolidation of capillary lumens by extracellular matrix and multiple synechiae (arrows). Some parietal epithelium and podocytes are hypertrophied. **Figure 10.** Hematoxylin and eosin. **Figure 11.** Periodic acid–Schiff reaction. **Figure 12.** There is moderate periglomerular fibrosis (*). Masson trichrome. **Figure 13.** Jones methenamine silver. **Figure 14.** Glomerulus from the same dog. There is global effacement of podocyte foot processes (arrowheads) and swelling of podocyte cytoplasm such that the urinary space cannot be identified. Bar = 2 μ m. Transmission electron microscopy. **Figure 15.** Immunofluorescence for IgG is negative.

and did not take up silver with the JMS method. Endocapillary hypercellularity was not present in any case. When present, mesangial hypercellularity was mild. Small synechiae were present in all cases and, in 1 case, involved all glomeruli. Interstitial changes were variable and mild, consisting of interstitial edema, interstitial amyloid, and amyloid deposition within vessel walls. Small amounts of amyloid were observed in the renal interstitium in 7 of the 12 cases, 4 of which also had rare amyloid deposits in renal cortical vessels. An additional 2 cases had vascular amyloid without detectable interstitial deposits.

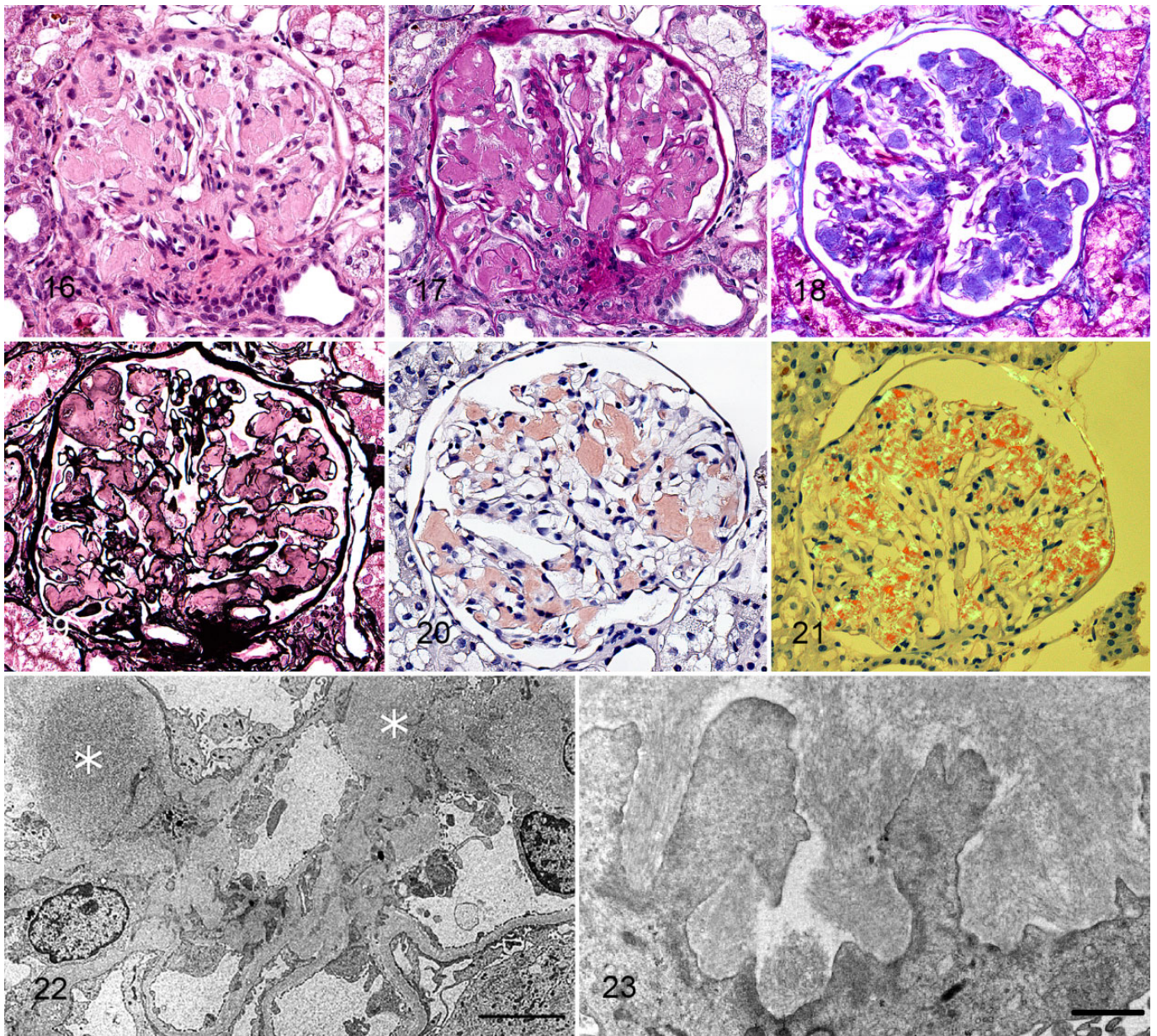
Ultrastructurally, all cases had amyloid deposition characterized by the presence of nonbranching fibrils (8- to 15-nm diameters) within the mesangium and capillary wall, predominantly in subendothelial and mesangial locations (Figs. 22, 23). Foot process effacement was a consistent finding. Electron-dense deposits were not present ultrastructurally. IF labeling revealed occasional equivocal labeling with all immunoreactants (Table 5).

As a group, dogs with amyloidosis did not have higher UPC or SCr values or lower SALb values than dogs in other proteinuric clusters (Table 6). Median UPC values from clusters 2, 3, 6, and 7 were lower than the median value from dogs with amyloidosis, whereas the median UPC values of clusters 5 and

8 were higher. Furthermore, 3 clusters of dogs had higher median SCr values, and 4 clusters of dogs had lower median SALb values than dogs with amyloidosis. Of note, however, dogs with amyloidosis were hypertensive less frequently than the dogs in any other cluster.

Immune Complex–Mediated Diseases

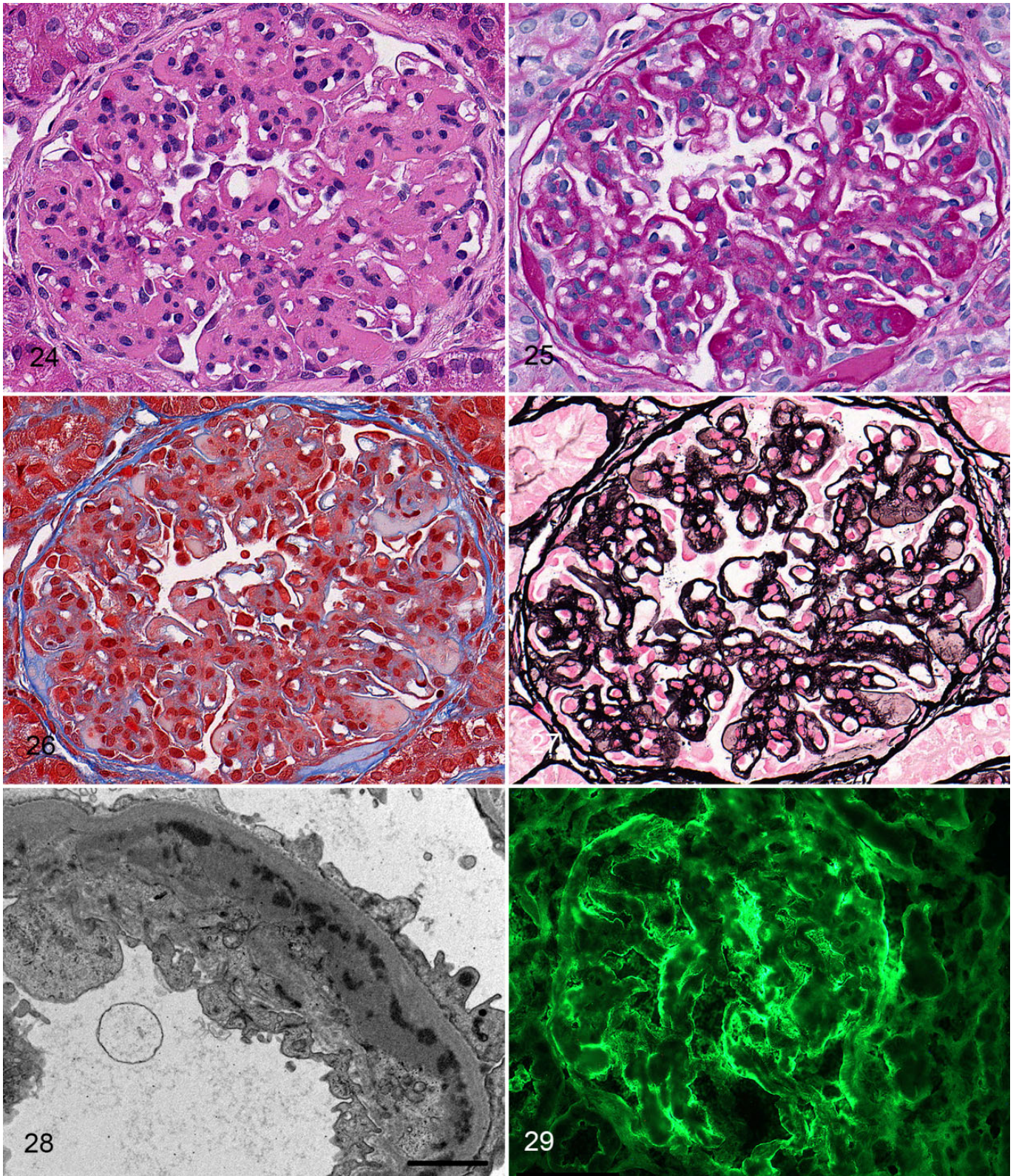
Membranoproliferative glomerulonephritis. Of the 89 cases, 23 (26%) grouped into cluster 5 (10 cases) and cluster 6 (13 cases) and had a glomerular pattern characteristic of MPGN. The defining LM feature of MPGN was glomerular endocapillary hypercellularity, characterized by increased numbers of cells (leukocytes, endothelial cells, and/or interposed mesangial cells) internal to the GBM with resultant encroachment or obliteration of peripheral capillary lumens. This endocapillary hypercellularity was global, diffuse, and often accompanied by mesangial hypercellularity (Figs. 24–27). Glomerular lesions that were more frequent in clusters 5 and 6 compared to other clusters were presence of neutrophils, duplication of GBMs, nuclear debris, parietal cell hypertrophy, and tubular regeneration. Small numbers of neutrophils (typically, 1–5 per glomerulus) were present in most glomeruli in all but 1 case;



Figures 16–23. Glomerular amyloidosis, dog, cluster 4. **Figure 16.** There is expansion of the mesangium by eosinophilic material. Hematoxylin and eosin. **Figure 17.** The material appears waxy pink. Periodic acid–Schiff reaction. **Figure 18.** The material is mottled blue to peach. Masson trichrome. **Figure 19.** The material does not take up silver. Jones methenamine silver. **Figure 20.** The material is congophilic. Congo red. **Figure 21.** The material demonstrates apple green birefringence. Congo red viewed with polarized light. **Figure 22.** Glomerulus from the same dog. The mesangium is expanded by amorphous electron-dense material (*). Bar = 5 μ m. Transmission electron microscopy. **Figure 23.** Higher magnification of the same glomerulus demonstrates amyloid fibrils organized into spikelike projections along capillary wall. There is podocyte foot process effacement. Bar = 1 μ m. Transmission electron microscopy.

specifically, they were present in up to 91% of examined glomeruli. Cluster 5 had LM parameters that were greater in intensity or prevalence than those in cluster 6, including synechia, GBM hyalinosis, afferent and efferent arteriolar hyalinosis, parietal cell proliferation, splitting of Bowman capsule, and periglomerular fibrosis. Two tubulointerstitial parameters were more common in cluster 5 than in cluster 6: interstitial fibrosis and inflammation.

The major ultrastructural features that distinguished clusters 5 and 6 from other clusters were the presence of prominent sub-endothelial and mesangial electron-dense deposits in 23 of 23 cases and 20 of 23 cases, respectively (Fig. 28). Other TEM features commonly identified in clusters 5 and 6 were mesangial cell interpositioning and endothelial cell swelling with lumen effacement. Prominent subepithelial electron-dense deposits were present in 1 of 10 cases in cluster 5 and 8 of



Figures 24–29. Membranoproliferative glomerulonephritis, dog, cluster 5. **Figures 24, 25.** There are global mesangial hypercellularity and segmental endocapillary hypercellularity. Capillary lumens are compressed by the expanded mesangium, thickened glomerular basement membrane (GBM), swollen endothelial cells, and interposed mesangial cells. **Figure 24.** Hematoxylin and eosin. **Figure 25.** Periodic acid–Schiff reaction. **Figure 26.** There is peach to orange material in the mesangium and capillary walls (hyalinosis). Masson trichrome. **Figure 27.** There are double contours of the GBM. Small synechiae are present. Jones methenamine silver. **Figure 28.** Glomerulus from the same dog. The GBM is

13 cases in cluster 6. These subepithelial deposits were often associated with GBM remodeling. Seven cases in cluster 6 had ultrastructural evidence of GBM spikes and encircled deposits, while 3 cases in cluster 5 had evidence of encircled deposits with no observable GBM spikes. As these cases with subepithelial electron-dense deposits shared the defining LM lesions and prominent subendothelial deposits of MPGN, they were considered a variant of MPGN (“mixed MPGN”).

While unequivocal positive labeling for IgA was not observed in any cases in clusters 5 and 6, clear positive labeling was observed in the capillary wall and/or mesangium for IgG, IgM, and/or C3 in all cases (Fig. 29). There were no significant differences in the IF patterns of all immunoglobulins and C3 between the 2 clusters.

As a group, dogs in cluster 5 had somewhat higher median UPC and SCr values and lower median SALb values than dogs did in cluster 6 (Table 6). These observations suggested a trend toward more severe clinical manifestations of disease for dogs in cluster 5 compared with those in cluster 6. However, the ranges of observed values for these variables among dogs in both clusters overlapped so much that it was impossible to discriminate dogs in these 2 clusters from each other based on these clinical observations. Of note, hypertension was very frequent in these groups; hypertension was more frequent among dogs in clusters 5 and 6 than among the dogs in any other cluster.

Membranous glomerulonephropathy. Of the 89 cases, 23 (26%) grouped into clusters 7 (13 cases) and 8 (10 cases) and had a glomerular pattern characteristic of MGN. Endocapillary hypercellularity was absent to minimal, except for 1 case in which it was scored as moderate. This parameter clearly distinguished the MGN pattern from the MPGN pattern but did not distinguish MGN clusters from non-ICGN clusters, which also lacked endocapillary hypercellularity (Table 1). Mesangial hypercellularity was minimal to mild in most MGN cases, wherein 3 to 5 mesangial cells per segment were commonly seen in 20 of 23 cases. By LM, most cases of MGN were associated with remodeling of the GBM, consisting of spikes radiating outward from the abluminal surface and/or holes within a thickened GBM (Figs. 30–33). Remodeling was more frequent and more prominent in cluster 7 compared with cluster 8. Red (fuchsinophilic) nodular deposits, suggestive of immune complexes and visible on the TRI stain, were observed via LM in 22 of 23 cases (Fig. 32); however, the deposits were scored as rare in 5 of these 22 cases. Red nodular deposits observable via LM were more prominent in the MGN pattern compared with the MPGN pattern. Importantly, capillary wall thickening was not specific for the MGN pattern, as this feature was also present in other clusters. Significant differences in lesions were noted between clusters 7 and 8 (Tables 1 and 2). Cases in cluster 7 had more severe GBM remodeling associated with subepithelial immune deposits than did cases in cluster 8, suggesting that

cluster 7 was associated with more chronic or severe disease. Both synechiae and secondary segmental glomerulosclerosis were significantly more common and/or more severe in cluster 7 compared with cluster 8. Hyalinosis of the GBM was mild in cluster 7 and minimal in cluster 8. Although synechiae, segmental glomerulosclerosis, and hyalinosis were helpful in delineating cluster 7 from cluster 8, they were also very prominent features of the FSGS and MPGN patterns (Table 1). Interstitial fibrosis was more common in cluster 7 compared with cluster 8. Generally, tubulointerstitial lesions did not differentiate the MGN pattern from other patterns, except for tubular epithelial cell isometric vacuolation, which was more frequent in cluster 8 when compared with all other clusters.

The defining feature of the MGN pattern was the presence of predominantly subepithelial electron-dense deposits on TEM. Electron-dense deposits and GBM changes induced by deposits were usually regularly spaced along the abluminal surface of at least 1 capillary loop in 22 of 23 cases, whereas the last case had ultrastructural evidence of dissolution of the deposits with only rare electron-dense deposits remaining. Although all MGN cases had subepithelial deposits observed ultrastructurally, red nodular deposits (TRI) were rare or absent via LM in 6 of these cases. Ultrastructural evidence of GBM remodeling (Fig. 34) was observed in 22 of 23 cases. In addition to prominent subepithelial deposits and GBM remodeling on TEM, 7 of the 23 cases also had subendothelial deposits. Despite the presence of subendothelial deposits, the absent to minimal endocapillary hypercellularity observed via LM in all but 1 MGN case separated them from the MPGN pattern. These cases were considered to be a variant of the membranous pattern “mixed MGN.”

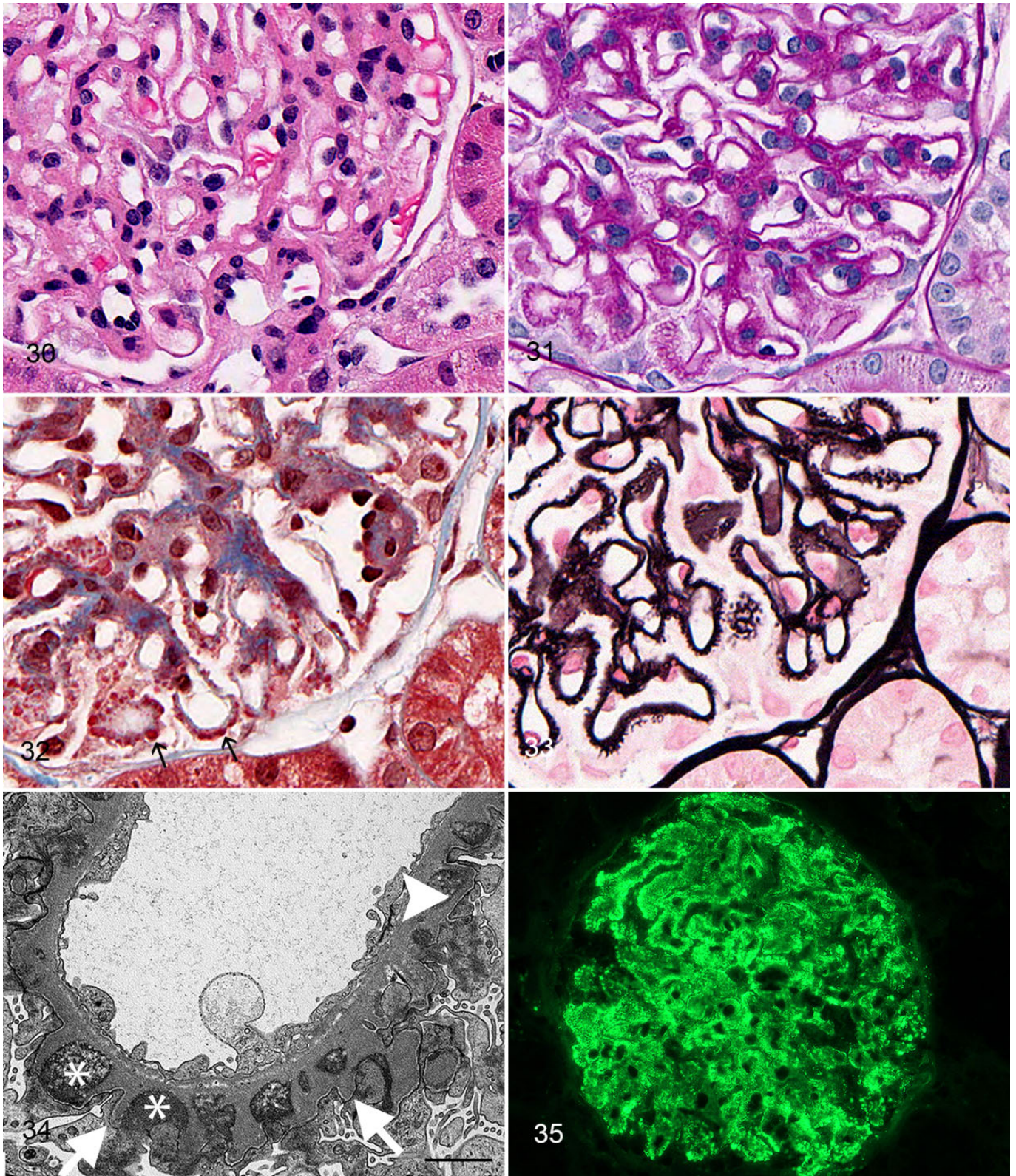
IF (Fig. 35) revealed unequivocal granular staining patterns for IgG, IgM, and C3 within the mesangium and along the GBM in all cases. Similar IF staining patterns were present in cases of the MPGN pattern and could not be used to differentiate between these 2 classes of immune complex-mediated glomerulonephritides.

As a group, dogs in cluster 8 had somewhat higher median UPC values and were more frequently hypertensive than those in cluster 7; however, the median SCr and SALb values for dogs in these 2 clusters were similar (Table 6).

Clinical Observations

Detailed analyses of clinical and laboratory parameters associated with the various patterns of canine glomerular injury included in this study were beyond the scope of this investigation. Nonetheless, key clinical variables were examined to provide a starting point for ongoing and future research that will include a larger number of affected dogs. Several potentially useful observations were made, which will require verification and further study to define their clinical utility. One was that

Figure 28. (continued) thickened due to the presence of variably electron-dense deposits in a subendothelial location. There is endothelial swelling and podocyte foot process effacement. Bar = 2 μ m. Transmission electron microscopy. **Figure 29.** Immunofluorescence for IgG shows unequivocal granular staining along capillary loops and mesangium.



Figures 30–35. Membranous glomerulonephropathy, dog, cluster 7. **Figures 30, 31.** There is mild segmental mesangial hypercellularity and moderate thickening of the capillary walls. Podocytes are markedly hypertrophied. **Figure 30.** Hematoxylin and eosin. **Figure 31.** Periodic acid–Schiff reaction. **Figure 32.** There are regularly spaced red nodules along the abluminal surface of the capillary walls, consistent with immune deposits (arrows). Masson trichrome. **Figure 33.** There are “spikes” and “holes” along the abluminal surface. Jones methenamine silver. **Figure 34.** Glomerulus from the same dog. There are numerous electron dense deposits (*) on the abluminal surface of the capillary wall, some of

the magnitude of proteinuria (ie, UPC values) did not discriminate among different clusters of affected dogs (Table 6). Second, dogs with the MPGN pattern of injury (clusters 5 and 6) had the most severe constellation of associated clinical abnormalities: their median UPC values were as high or higher and their median SALb values, as low or lower, than those of dogs in other clusters. Also, dogs with MPGN had higher median SCr values and hypertension more often than dogs in any other clusters. Third, although dogs with glomerulosclerosis (clusters 2 and 3) generally had the least severe constellation of clinical abnormalities (lower median UPC and SCr values and higher median SALb values than those of dogs in other clusters, with hypertension only moderately often), the ranges of clinical data were large (Table 6). Finally, dogs with amyloidosis (in cluster 4) were hypertensive less often than dogs in any other cluster, but they were otherwise more comparable to dogs with MGN (in clusters 7 and 8) than to dogs in any other clusters.

Discussion

The purpose of this project was to objectively formulate a prototype scheme for classification of glomerular diseases in proteinuric dogs.¹³ While the human World Health Organization classification system for glomerular disease has been used to evaluate canine kidneys, the validity of adopting the human classification scheme for canine patients has not been assessed. Eight veterinary pathologists graded 114 parameters representing a wide array of glomerular, tubulointerstitial, and vascular lesions examined with LM, TEM, and IF. The data set was analyzed by hierarchical cluster analysis, which enabled the development of an objectively derived prototype classification scheme. With this scheme now developed, a larger number of cases will be studied in the next phase to validate the classification system and to correlate pathologic findings with clinical and laboratory parameters and patient outcome.

The method of hierarchical cluster analysis, which included Ward's linkage and L2 dissimilarity, works particularly well for the data set created for this study because it performs best with clearly defined clusters and when there are few outliers.³⁹ The greatest dissimilarity among clusters is present at the top of the dendrogram, where 2 distinct clusters emerged separating the patterns of predominantly non-immune complex glomerular diseases (normal, amyloid, and FSGS) from patterns of immune complex glomerular diseases (MPGN and MGN). Typically, a bar parallel to the *x*-axis is drawn to denote the number of clusters at a particular level of dissimilarity. For our evaluation, a bar that delineates 8 clusters was drawn, 7 of which were distinguishable from the control cluster.

While these 8 clusters encompass the most commonly observed patterns of glomerular lesions seen in dogs, there are a number of specific but uncommon diagnoses that were

excluded from cluster analysis. In fact, after a preliminary dendrogram was created, 7 cases with seemingly rare diagnoses were identified and excluded from analysis. Cluster analysis is an iterative process in which the investigator attempts to find a dendrogram pattern that makes physiologic (or pathophysiologic) sense. Exclusion of these 7 cases that appeared to be outliers resulted in a dendrogram that could be more cogently interpreted.

FSGS is a common morphologic pattern of glomerular disease in humans with the nephrotic syndrome and is due to injury to the glomerular visceral epithelial cell (podocyte). The podocyte plays a central role in glomerular filtration permselectivity and responds to injury with reversible changes of hypertrophy, foot process effacement, cell body attenuation, and microvillus formation.²¹ With continued injury, the podocyte irreversibly detaches from the outer aspect of the GBM. Since the podocyte is a terminally differentiated cell with minimal proliferative capability, podocyte loss results in hypertrophy of the remaining podocytes to cover the denuded GBM. Experimental data indicate that if >40% of the podocytes are lost, the remaining podocytes are unable to cover the entire tuft.⁵¹ Denuded areas of GBM adhere to Bowman capsule (synechiae), and the tuft undergoes segmental sclerosis or scarring.

Podocyte loss and FSGS may be primary or secondary. Primary (or idiopathic) FSGS is assumed to be due to innate defects in podocyte or slit diaphragm genes or proteins. In humans, once a causative mutation is identified and the pathogenesis of podocyte injury is elucidated, then that type of FSGS is considered to be secondary, which is discussed below. While primary FSGS is a common morphologic pattern of glomerular disease in people with the nephrotic syndrome, it has only recently been recognized in dogs. Well-documented primary canine FSGS—with histopathologic, IF, and electron microscopic findings similar to the cases in this study—was first described in 2010.³ With the advent of improved renal diagnostics, the lesion of primary FSGS has recently been recognized as a common cause of glomerular disease in dogs. In a larger retrospective study that included cases used in this project, LM, IF, and TEM evaluation of canine renal disease showed that FSGS was a common cause of proteinuria, accounting for 20.6% of the cases. In that group of dogs, FSGS was more common than amyloidosis, which accounted for only 15.2% of the cases.⁴⁰ Recently, genome-wide association studies of protein-losing nephropathy of Soft-Coated Wheaten Terriers revealed mutations in 2 genes, *NPHS1* and *KIRREL2*, encoding nephrin and filtrin, respectively. These proteins are part of the podocyte slit diaphragm, and FSGS is the dominant pathologic phenotype in proteinuric Soft-Coated Wheaten Terriers; however, the exact pathogenesis of how these mutations interfere with podocyte function remains unknown.²⁶ Similar genetic causes of primary/familial FSGS have been identified in humans.

Figure 34. (continued) which have a moth-eaten appearance indicative of dissolution. Deposits are separated by spikes (arrows) or encircled by the glomerular basement membrane (arrowhead). Podocyte foot processes are globally effaced, and microvillus transformation of podocyte cytoplasm is prominent. Bar = 2 μ m. Transmission electron microscopy. **Figure 35.** Immunofluorescence for IgG shows unequivocal granular staining along capillary loops.

Secondary (or adaptive) FSGS is well recognized in dogs with decreased functional renal mass associated with naturally occurring chronic renal disease or following experimental partial nephrectomy⁷ and, until relatively recently, was thought to be the only form of FSGS occurring in dogs. In this type of secondary FSGS, decreased renal mass leads to glomerular hypertrophy and glomerular hyperfiltration of the remaining nephrons. While these glomerular changes are initially adaptive responses that increase glomerular filtration rate, they eventually become maladaptive, causing podocyte injury, podocyte detachment, and eventually glomerulosclerosis. Dogs with 11/12 nephrectomy and secondary glomerulosclerosis are azotemic (SCr, 2.0–2.5 mg/dl) and mildly proteinuric (mean UPC <0.8),⁸ in contrast to the variable occurrence of azotemia and more profound proteinuria observed in dogs with primary FSGS. Similar pathogenesises are likely occurring in cases of congenital nephron paucity, as in dogs with juvenile-onset nephropathies.

Secondary FSGS may also be caused by other types of injury to the podocyte.³⁶ Immune complex glomerulonephritis can induce podocyte injury and secondary segmental glomerulosclerosis in humans and dogs, which leads to a diagnostic dilemma. Cases with segmental sclerosis evaluated solely with LM might have histologically undetectable immune complex deposits in the capillary walls for which immunosuppression would be recommended, emphasizing the importance of TEM and IF. Hypertension is also known to injure podocytes and cause FSGS in humans and might have a similar effect in some dogs.¹⁴ Although obesity and hypertension have been associated with proteinuria in dogs,^{4,48} other studies have found conflicting results.⁴⁶ It is important to realize that renal tissue was not consistently evaluated with advanced diagnostic modalities in those veterinary studies, so the association of hypertension and obesity with FSGS requires further investigation.

All dogs in the FSGS group had similar lesions histologically, with increased severity of lesions in cluster 3 compared with cluster 2. Cases in cluster 3 had a significantly greater percentage of glomeruli with sclerosis and significantly more synechiae as compared with cluster 2. GBM hyalinosis, characterized by insudation of plasma lipoproteins into the damaged capillary wall, and obsolescent glomeruli were also more prevalent in cluster 3. The coexistence of glomerular lipidosis encountered only among cases of FSGS (clusters 2 and 3) was also noted. Glomerular lipidosis in dogs has most often been reported as a sporadic, incidental glomerular change in kidneys that otherwise lack significant pathology.^{47,55} This association between glomerular lipidosis and FSGS may change as larger numbers of cases are eventually considered, but its occurrence in a small number of FSGS cases in this study suggests that glomerular lipidosis may have pathologic significance. Future studies of the lesion of glomerular lipidosis in dogs are warranted.

Seven cases within the FSGS group were exceptions to the ICGN versus non-ICGN division of the dendrogram, because TEM revealed the presence of electron-dense deposits. Review of these cases revealed that although electron-dense material consistent with immune deposits was observed in the mesangium, involvement of the capillary walls was absent or rare.

The significance of having electron-dense deposits limited to the mesangial regions is unknown; however, it is clear that the histopathologic pattern is one of mesangial expansion, mesangial hypercellularity, and segmental sclerosis, as opposed to endocapillary hypercellularity and remodeling of the GBM. These 7 cases might represent primary FSGS with secondary nonspecific trapping of plasma constituents. Recent research in mice and humans has suggested that non-immune-mediated injury to the glomerulus can entrap circulating IgM, which can subsequently activate the complement system leading to progressive glomerular injury.⁴³ Alternatively, these 7 cases could represent a sclerosing response of the glomerulus secondary to previous mesangial deposition of immune complexes, similar to what occurs in the sclerosing phenotype of mesangioproliferative IgA or C1q glomerulopathy in humans.^{30,53} Given that glomerulosclerosis, an irreversible lesion, was prominent in these 7 cases whereas the electron-dense deposits were less so, it is justifiable to keep these cases in the FSGS cluster. However, the presence of these electron-dense deposits might exacerbate glomerular injury, and immunosuppressive therapy might be a consideration in situations where standard therapies are unsuccessful.

The FSGS pattern raises 3 important points. First, FSGS is sufficient to result in proteinuria, which can sometimes be severe. Second, because this disease begins as a focal process, every glomerulus in a renal biopsy specimen should be examined. In humans, approximately 20 to 25 glomeruli need to be evaluated to confidently rule out this diagnosis.¹⁸ Third and most important, the correct diagnosis of this lesion is crucial for the assessment of potential treatment options.

Glomerular amyloidosis is not typically a diagnostic dilemma, although occasional cases will have only minimal amyloid deposits. In these situations, the diagnosis will rest on the detection of small aggregates of fibrils with TEM and negative IF results.

The ICGN branch of the dendrogram comprised 4 clusters, 2 of which had MPGN patterns and 2 of which had MGN patterns. MPGN is a pattern characterized by the presence of endocapillary hypercellularity and double contours of the GBM. With rare exception (discussed below), both lesions are due to the presence of subendothelial immune complexes. Theories have been proposed for the pathogenesis of immune complex deposition, ranging from entrapment of circulating immune complexes to entrapment of a nonglomerular antigen in the subendothelial space, followed by eventual interaction with circulating antibody.³⁴ Regardless of how they are deposited beneath the endothelium, it is their ability to activate the complement cascade in proximity to the capillary lumen that results in a hypercellular appearance. It is important to distinguish endocapillary hypercellularity from mesangial hypercellularity when evaluating glomeruli. Endocapillary hypercellularity consists of increased numbers of circulating inflammatory cells with hypertrophied or hyperplastic endothelial cells and/or interposed mesangial cells within peripheral capillaries. In contrast, mesangial cell proliferation is confined to the central mesangial matrix. Confusion arises because endocapillary hypercellularity and mesangial cell proliferation are not

mutually exclusive lesions and because evaluation of 5- μ m-thick sections leads to overestimation of the number of nuclei within a segment of the glomerular tuft. Use of the PAS reaction and JMS method enabled the pathologists to readily determine the location of the hypercellularity.

The PAS reaction and JMS method also allowed the pathologists to discern between GBM thickening and definitive double-membrane contours, which are the result of synthesis of new GBM material by the glomerular endothelium. The use of TEM and IF verified the presence of immune complexes, thereby justifying a diagnosis of MPGN. Importantly, there are diseases that have a histologic pattern resembling MPGN but lack immune complexes. Examples in humans include thrombotic microangiopathy,¹⁹ fibrillary glomerulonephritides,¹ and C3 glomerulopathy.^{6,41} Of these, thrombotic microangiopathy⁹ and C3 glomerulopathy have been reported in veterinary species.^{2,5,37} IF and TEM are needed to differentiate immune complex MPGN from these rare diseases with alternate pathogeneses, because therapy and prognosis depend on the correct diagnosis.

MGN is a pattern of injury caused by the presence of immune complexes on the subepithelial (abluminal) side of the GBM. The presence of a thickened GBM is insufficient to warrant this diagnosis. This represents a distinct shift from the era in which MGN was diagnosed solely on the LM appearance of a thick capillary wall. In the pattern of MGN proposed by the current study, the immune complexes induce production of new GBM next to deposits (giving the appearance of spikes), which eventually become encircled by new GBM. The encircled deposits take on the appearance of clear holes when viewed by LM sections prepared by the JMS method. Therefore, GBM remodeling (spikes or holes) is a more important histologic finding than thickened capillary walls. Because subepithelial immune complexes are separated from the capillary lumen by GBM, endocapillary hypercellularity is minimal to nonexistent. One feature that separated clusters 7 and 8 was the presence of segmental sclerosis, which is presumed to be secondary to podocyte injury driven by the subepithelial immune complexes. The subepithelial immune complexes activate complement, causing podocyte injury with podocyte foot process effacement and increased loss of podocytes via C5b-9-mediated cellular injury.³⁵ Secondary segmental glomerulosclerosis has prognostic significance in humans,³⁵ and a similar relationship might eventually be identified in dogs.

Cases from clusters 5 and 8 were more severely affected (ie, had more severe lesions) than clusters 6 and 7, respectively. This might represent a greater impetus for immune complex deposition or different stages of the diseases. Future studies will investigate the relationship among underlying systemic diseases, which could be a source of antigenemia. We did not detect significant associations between the composition of immune complex deposits as shown by the IF labeling and the various patterns of histologic and ultrastructural lesions demonstrated by the LM and TEM findings. Of interest, IgA staining was infrequent to rare (as opposed to the frequency of IgA nephropathy in humans). We also did not identify cases

of C3-only staining, which would be supportive of a C3 glomerulopathy.⁶ That does not mean that these types of glomerular diseases do not exist in dogs but merely that they were not identified in our cohort of 89 cases. It remains necessary to perform a panel of IF staining so that uncommon or rare diseases can be identified and properly investigated.

It is possible that the ICGN might represent a spectrum ranging from a pure membranous form—with only subepithelial immune complexes and lacking hypercellularity—to a pure membranoproliferative form with immune complexes located solely in a subendothelial location and associated with fulminate inflammatory cell accumulation. The middle portion of the spectrum may have both subepithelial and subendothelial immune complex deposition with varying degrees of endocapillary hypercellularity. In fact, this middle ground was previously diagnosed as type III MPGN (Burkholder variant) in humans and dogs. The World Health Organization classification of glomerular disease in humans is currently in a state of reorganization, with the recent identification of complementopathies and associated C3 glomerulopathies⁴¹ as well as with the development of the International Society for Nephrology / Renal Pathology Society proposal for classification of lupus nephritis.²⁹ This calls into question the validity of adopting terminology such as type III MPGN from human nephropathology, when it is rarely used and considered controversial. Therefore, we were very interested in how cases with deposits in multiple locations would cluster in our cohort. Cluster analysis did not separate out these “mixed cases” from purer patterns, thus suggesting that the ultrastructural localization of ICs was not a driving force for cluster grouping in this particular cohort of patients. Determining whether or not canine cases will eventually be associated with an underlying infection, complementopathy, or autoimmune disease is a future goal of this initiative. It is possible that the variation in immune complex location will have etiologic or prognostic implications. Therefore, we have opted to diagnose these cases as mixed MPGN and mixed MGN so that the clinical presentation, progression, and outcome of these “variants” can be investigated.

Notably, cluster analysis based solely on the LM features of glomeruli resulted in a strikingly different dendrogram with many misclassified cases. Seven of the 8 MGN cases in cluster 8 incorrectly clustered with dogs without evidence of immune complex deposition. Reexamination of these cases revealed fewer spikes and holes on the silver stain and only mildly thickened GBMs. This demonstrates that GBM remodeling can be subtle or absent in early cases of MGN and emphasizes the importance of additional modalities for the correct diagnosis. Likewise, all of the cases from cluster 3 (FSGS) were incorrectly clustered with ICGN cases, likely because FSGS cases may have mesangial hypercellularity and thickened capillary walls. Evaluating renal biopsies solely by LM can introduce significant errors that would have adverse therapeutic and prognostic implications. Moreover, this clearly illustrates the importance of TEM and IF for the correct classification of canine glomerular disorders.

Table 7. Diagnostic Criteria for 5 Common Categories of Glomerular Disease Based on Evaluation of 89 Proteinuric Dogs.^a

Focal segmental glomerulosclerosis: clusters 2 and 3	
LM	Solidification of a portion of the capillary tuft by extracellular matrix
TEM	Extensive effacement of podocyte foot processes ± Few to rare electron dense deposits (mostly mesangial) observed in some cases
IF	Lack of granular staining with antibodies against IgG, LLC, and C3
Amyloidosis: cluster 4	
LM	Variable degree of mesangial expansion by congophilic material that exhibits apple green birefringence when examined with polarized light; material is pale pink with PAS and blue to peach with TRI and does not take up silver with the JMS method
TEM	Fibrils (8- to 15-nm diameters) within the mesangium and capillary walls
IF	Lack of granular staining with antibodies against IgG, LLC, and C3
Membranoproliferative glomerulonephritis: clusters 5 and 6	
LM	Global diffuse endocapillary and mesangial hypercellularity ± Double contours of the GBM (best seen with JMS and PAS)
TEM	Subendothelial and mesangial electron-dense deposits ± Subepithelial electron-dense deposits (referred to as mixed MPGN in text)
IF	Granular staining along capillary loops with antibodies against IgG, LLC, and C3
Membranous glomerulonephropathy: clusters 7 and 8	
LM	Histologic appearance varies depending on time frame of disease, but endocapillary hypercellularity is absent. ± Mild mesangial hypercellularity; regularly spaced red nodules along the subepithelial aspect of the GBM (noted on TRI); “spikes” on the subepithelial surface and “holes” within the capillary walls (best seen with JMS)
TEM	Subepithelial electron-dense deposits with or without deposits in the mesangium ± “Spikes” in between electron-dense deposits; encircled electron-dense deposits; regularly spaced electron lucencies indicates reabsorption of deposits; subendothelial electron-dense deposits (referred to as mixed MGN in text)
IF	Granular staining along capillary loops with antibodies against IgG, LLC, and C3 Cases in which deposits have been reabsorbed will have minimal positive staining.

Abbreviations: C3, complement component 3; GBM, glomerular basement membrane; IF, immunofluorescence; IgG, immunoglobulin G; JMS, Jones methenamine silver; LLC, lambda light chain; LM, light microscopy; PAS, Periodic acid Schiff; TEM, transmission electron microscopy; TRI, Masson trichrome.

^aPlanned future studies might lead to modification of criteria and will include less common categories of glomerular disease. Parameters that were observed in multiple diagnostic categories (eg, hyalinosis) are not included.

A limitation of this study was that the collection of renal biopsy material from control dogs was difficult, as it is an invasive procedure. Therefore, we used tissue obtained during ovariohysterectomy prior to adoption of racing Greyhounds, which precluded any breed or age matching with the case cohort. Additionally, certain clinical parameters—such as signalment, body condition score, and infectious disease exposure—were not examined in this study, as those data will be analyzed in future publications from the veterinary nephrologists associated with the WSAVA-RSSG.

The question arises whether classification of these lesions by evaluation of a large number of morphologic parameters is worth the additional effort. Clearly, the comparison of dendrogram in Figure 3 (only LM parameters) to that of Figure 2 (all modalities) demonstrates the necessity of advanced diagnostics. Using only LM features resulted in the misclassification that might have led to inappropriate treatment of 22 of 89 cases (25%). With the advent of immunosuppressive agents for ICGN, considerable care should be taken to determine which patients will likely benefit from these therapeutic regimens. It is also our opinion that valuable phenotypic data will be lost if the lesions are not clearly defined and quantified. This lesion-based

phenotypic approach could help better categorize cases for epidemiologic analyses, investigation of molecular pathogenesis, prognostication, and treatment decisions. A similar approach is the basis of the Nephrotic Syndrome Study Network (NEPTUNE) study, in which lesions identified in renal biopsy specimens of nephrotic human patients are accurately phenotyped for ongoing and future molecular tissue analysis.¹⁵

A number of the dogs in this study are part of an ongoing project designed to follow clinical progression of disease after assessment of their renal biopsy using this prototypical classification scheme. Biopsies of additional dogs enrolled in this prospective study will be similarly evaluated, and outcome data will be analyzed. The classification scheme that we propose in this study is intended to be modifiable when outcome data become available from these ongoing incident cohort studies. In its current form, however, our proposed clusters (Table 7) will facilitate communication among clinicians and pathologists, whereas our list of lesions will clarify the terminology used in histopathologic descriptions. With this scheme in hand, a larger number of cases (patients) will be studied in the next phase to validate the classification system and to correlate histologic findings with clinical and clinical laboratory parameters and outcomes.

Acknowledgements

We acknowledge the substantive contributions of Dr Brian R. Berbridge (Glaxo Smith Kline, Raleigh, NC, USA) and Dr Fred J. Clubb Jr (Department of Veterinary Pathobiology, Texas A&M University, College Station, TX, USA) to the conceptualization and initial planning of this project. Additionally, we gratefully thank Ralph Nichols (Texas Heart Institute, Houston, TX, USA) and Mary Sanders (Department of Small Animal Clinical Sciences, Texas A&M University, College Station, TX, USA), the staff of the Department of Pathobiology at Utrecht University, and the staff at the University of Padova for their expert technical assistance, without which this project could not have been completed.

This work was performed under the auspices of the World Small Animal Veterinary Association Standardization Projects program with generous financial support from Hill's Pet Nutrition and from Bayer Animal Health.

Authors' Note

Research materials can be accessed by contacting the first author, R. E. Cianciolo.

Declaration of Conflicting Interests

The author(s) declared no potential conflicts of interest with respect to the research, authorship, and/or publication of this article.

Funding

The author(s) received no financial support for the research, authorship, and/or publication of this article.

References

- Alpers CE, Kowalewska J. Fibrillary glomerulonephritis and immunotactoid glomerulopathy. *J Am Soc Nephrol*. 2008;**19**(1):34–37.
- Angus KW, Gardiner AC, Mitchell B, et al. Mesangiocapillary glomerulonephritis in lambs: the ultrastructure and immunopathology of diffuse glomerulonephritis in newly born Finnish Landrace lambs. *J Pathol*. 1980;**131**(1):65–74.
- Aresu L, Zanatta R, Luciani L, et al. Severe renal failure in a dog resembling human focal segmental glomerulosclerosis. *J Comp Pathol*. 2010;**143**(2–3):190–194.
- Bacic A, Kogika MM, Barbaro KC, et al. Evaluation of albuminuria and its relationship with blood pressure in dogs with chronic kidney disease. *Vet Clin Pathol*. 2010;**39**(2):203–209.
- Blum JR, Cork LC, Morris JM, et al. The clinical manifestations of a genetically determined deficiency of the third component of complement in the dog. *Clin Immunol Immunopathol*. 1985;**34**(3):304–315.
- Bomback AS, Appel GB. Pathogenesis of the C3 glomerulopathies and reclassification of MPGN. *Nat Rev Nephrol*. 2012;**8**(11):634–642.
- Brown SA, Crowell WA, Brown CA, et al. Pathophysiology and management of progressive renal disease. *Vet J*. 1997;**154**(2):93–109.
- Brown SA, Finco DR, Brown CA, et al. Evaluation of the effects of inhibition of angiotensin converting enzyme with enalapril in dogs with induced chronic renal insufficiency. *Am J Vet Res*. 2003;**64**(3):321–327.
- Carpenter JL, Andelman NC, Moore FM, et al. Idiopathic cutaneous and renal glomerular vasculopathy of greyhounds. *Vet Pathol*. 1988;**25**(6):401–407.
- Center SA, Smith CA, Wilkinson E, et al. Clinicopathologic, renal immunofluorescent, and light microscopic features of glomerulonephritis in the dog: 41 cases (1975–1985). *J Am Vet Med Assoc*. 1987;**190**(1):81–90.
- Cianciolo RE, Brown CA, Mohr FC, et al. Pathologic evaluation of canine renal biopsies: methods for identifying features that differentiate immune-mediated glomerulonephritides from other categories of glomerular diseases. *J Vet Intern Med*. 2013;**27**:S10–S18.
- Cook AK, Cowgill LD. Clinical and pathological features of protein-losing glomerular disease in the dog: a review of 137 cases (1985–1992). *J Am Anim Hosp Assoc*. 1996;**32**(4):313–322.
- Cowgill LD, Polzin DJ. Vision of the WSAVA Renal Standardization Project. *J Vet Intern Med*. 2013;**27**:S5–S9.
- D'Agati VD. The spectrum of focal segmental glomerulosclerosis: new insights. *Curr Opin Nephrol Hypertens*. 2008;**17**(3):271–281.
- Gadegbeku CA, Gipson DS, Holzman LB, et al. Design of the Nephrotic Syndrome Study Network (NEPTUNE) to evaluate primary glomerular nephropathy by a multidisciplinary approach. *Kidney Int*. 2013;**83**(4):749–756.
- Harris CH, Krawiec DR, Gelberg HB, et al. Canine IgA glomerulonephropathy. *Vet Immunol Immunopathol*. 1993;**36**(1):1–16.
- Jaenke RS, Allen TA. Membranous nephropathy in the dog. *Vet Pathol*. 1986;**23**(6):718–733.
- Jennette JC, Olson J, Schwartz M, et al. Primer on the pathologic diagnosis of renal disease. In: *Heptistall's Pathology of the Kidney*. 6th ed. Philadelphia, PA: Lippincott Williams & Wilkins; 2007:97–123.
- Keir L, Coward RJ. Advances in our understanding of the pathogenesis of glomerular thrombotic microangiopathy. *Pediatr Nephrol*. 2011;**26**(4):523–533.
- Koeman JP, Biewenga WJ, Gruys E. Proteinuria in the dog: a pathomorphological study of 51 proteinuric dogs. *Res Vet Sci*. 1987;**43**(3):367–378.
- Kriz W, Shirato I, Nagata M, et al. The podocyte's response to stress: the enigma of foot process effacement. *Am J Physiol Renal Physiol*. 2013;**304**(4):F333–F347.
- Kurtz JM, Russell SW, Lee JC, et al. Naturally occurring canine glomerulonephritis. *Am J Pathol*. 1972;**67**(3):471–482.
- Lees GE, Brown SA, Elliott J, et al. Assessment and management of proteinuria in dogs and cats: 2004 ACVIM Forum Consensus Statement (small animal). *J Vet Intern Med*. 2005;**19**(3):377–385.
- Lewis RJ. Canine glomerulonephritis: results from a microscopic evaluation of fifty cases. *Can Vet J*. 1976;**17**(7):171–176.
- Littman MP, Daminet S, Grauer GF, et al. Consensus recommendations for the diagnostic investigation of dogs with suspected glomerular disease. *J Vet Intern Med*. 2013;**27**(suppl 1):S19–S26.
- Littman MP, Wiley CA, Raducha MG, et al. Glomerulopathy and mutations in NPHS1 and KIRREL2 in soft-coated Wheaten Terrier dogs. *Mamm Genome*. 2013;**24**(3–4):119–126.
- Macdougall DF, Cook T, Steward AP, et al. Canine chronic renal disease: prevalence and types of glomerulonephritis in the dog. *Kidney Int*. 1986;**29**(6):1144–1151.
- Marino CL, Cober RE, Iazbik MC, et al. White-coat effect on systemic blood pressure in retired racing Greyhounds. *J Vet Intern Med*. 2011;**25**(4):861–865.
- Markowitz GS, D'Agati VD. The ISN/RPS 2003 classification of lupus nephritis: an assessment at 3 years. *Kidney Int*. 2007;**71**(6):491–495.
- Mii A, Shimizu A, Masuda Y, et al. Current status and issues of C1q nephropathy. *Clin Exp Nephrol*. 2009;**13**(4):263–274.
- Miyauchi Y, Nakayama H, Uchida K, et al. Glomerulopathy with IgA deposition in the dog. *J Vet Med Sci*. 1992;**54**(5):969–975.
- Muller-Peddinghaus R, Trautwein G. Spontaneous glomerulonephritis in dogs: I. Classification and immunopathology. *Vet Pathol*. 1977;**14**(1):1–13.
- Murray M, Wright NC. A morphologic study of canine glomerulonephritis. *Lab Invest*. 1974;**30**(2):213–221.
- Nangaku M, Couser WG. Mechanisms of immune-deposit formation and the mediation of immune renal injury. *Clin Exp Nephrol*. 2005;**9**(3):183–191.
- Nangaku M, Shankland SJ, Couser WG. Cellular response to injury in membranous nephropathy. *J Am Soc Nephrol*. 2005;**16**(5):1195–1204.
- Noël LH. Morphological features of primary focal and segmental glomerulosclerosis. *Nephrology Dialysis Transplantation*. 1999;**14**(suppl 3):53–57.
- Reusch C, Hoerauf A, Lechner J, et al. A new familial glomerulonephropathy in Bernese mountain dogs. *Vet Rec*. 1994;**134**(16):411–415.
- Rouse BT, Lewis RJ. Canine glomerulonephritis: prevalence in dogs submitted at random for euthanasia. *Can J Comp Med*. 1975;**39**(4):365–370.
- Sarstedt M, Mooi E. *A Concise Guide to Market Research: The Process, Data, and Methods Using IBM SPSS Statistics*. Berlin: Springer Verlag; 2011.

40. Schneider SM, Cianciolo RE, Nabity MB, et al. Prevalence of immune-complex glomerulonephritides in dogs biopsied for suspected glomerular disease: 501 cases (2007–2012). *J Vet Intern Med.* 2013;**27**(suppl 1): S67–S75.
41. Sethi S, Fervenza FC. Membranoproliferative glomerulonephritis: pathogenetic heterogeneity and proposal for a new classification. *Semin Nephrol.* 2011;**31**(4): 341–348.
42. Slauson DO, Lewis RM. Comparative pathology of glomerulonephritis in animals. *Vet Pathol.* 1979;**16**(2):135–164.
43. Strassheim D, Renner B, Panzer S, et al. IgM contributes to glomerular injury in FSGS. *J Am Soc Nephrol.* 2013;**24**(3):393–406.
44. Stuart BP, Plemister RD, Thomassen RW. Glomerular lesions associated with proteinuria in clinically healthy dogs. *Vet Pathol.* 1975;**12**(2):125–144.
45. Surman S, Couto CG, Dibartola SP, Chew DJ. Arterial blood pressure, proteinuria, and renal histopathology in clinically healthy retired racing greyhounds. *J Vet Intern Med.* 2012;**26**(6):1320–1329.
46. Tefft KM, Shaw DH, Ihle SL, et al. Association between excess body weight and urine protein concentration in healthy dogs. *Vet Clin Pathol.* 2014;**43**(2): 255–260.
47. Thiel W, Hartig F, Frese K. Glomerular lipidosis in the dog. *Exp Pathol.* 1981; **19**(3):154–160.
48. Tvarijonavičiute A, Ceron JJ, Holden SL, et al. Obesity-related metabolic dysfunction in dogs: a comparison with human metabolic syndrome. *BMC Vet Res.* 2012;**8**:147.
49. Vilafranca M, Wohlsein P, Leopold-Temmler B, et al. A canine nephropathy resembling minimal change nephrotic syndrome in man. *J Comp Pathol.* 1993;**109**(3):271–280.
50. Vilafranca M, Wohlsein P, Trautwein G, et al. Histological and immunohistological classification of canine glomerular disease. *J Vet Med Ser A.* 1994; **41**(1–10):599–610.
51. Wharram BL, Goyal M, Wiggins JE, et al. Podocyte depletion causes glomerulosclerosis: diphtheria toxin-induced podocyte depletion in rats expressing human diphtheria toxin receptor transgene. *J Am Soc Nephrol.* 2005;**16**(10):2941–2952.
52. Wright NG, Nash AS, Thompson H, et al. Membranous nephropathy in the cat and dog: a renal biopsy and follow-up study of sixteen cases. *Lab Invest.* 1981; **45**(3):269–277.
53. Wyatt RJ, Julian BA. IgA nephropathy. *N Engl J Med.* 2013;**368**(25):2402–2414.
54. Yhee JY, Yu CH, Kim JH, et al. Histopathological retrospective study of canine renal disease in Korea, 2003–2008. *J Vet Sci.* 2010;**11**(4):277–283.
55. Yayed I, Gopinath C, Hornstra HW, et al. A light and electron microscopical study of glomerular lipidosis in beagle dogs. *J Comp Pathol.* 1976;**86**(4): 509–517.